

Generalized proximity effect in metallic F/S/F heterostructures

V. Apinyan and R. Mélin*

Centre de Recherches sur les Très Basses Températures (CRTBT)[†]
CNRS BP 166X, 38042 Grenoble Cedex, France

We consider the theory of F/S/F heterostructures with metallic or insulating ferromagnetic electrodes, and find that the metallic heterostructure is controlled by a new physics related to a generalized proximity effect involving pair correlations among the two ferromagnets. The critical temperature of the superconductor with parallel spin orientations of the ferromagnetic electrodes is larger than the critical temperature of the superconductor with antiparallel spin orientations, which is opposite to the model for insulating ferromagnets first solved by de Gennes. We develop two complementary methods to solve a microscopic model and to find reliable determinations of the superconducting gap (a gap kernel approach and exact diagonalizations). We discuss in details the role of “phase disorder” and show that the microscopic phase variables should be antisymmetric. We show that the basic physics of the model can be understood by considering the lowest order non vanishing Feynman diagrams. The non local proximity effect can be characterized by a matrix of Gorkov functions which we calculate explicitly. With metallic ferromagnets, the diagrams involved in the renormalization of the superconducting order parameter (arising from energies above the superconducting gap) are identical to those involved in the non local proximity effect (arising from energies below the superconducting gap). Finally, we propose new experiments to test our theoretical prediction.

I. INTRODUCTION

It is well known since the work by Gennes in 1966 [1] that with *insulating ferromagnets* the superconducting transition temperature of a ferromagnet/ superconductor/ ferromagnet (F/S/F) trilayer is smaller if the ferromagnetic electrodes have a parallel spin orientation. Spin-up and spin-down electrons form evanescent waves in the insulating ferromagnets. The effect of the ferromagnets can then be treated as a perturbation [1]. As a result the single electron states in the superconductor are coupled to an effective exchange field. The effective exchange field cancels if the two ferromagnets have an antiparallel spin orientation. Because an exchange field in a superconductor is a pair-breaking perturbation, the transition temperature of the superconductor and the superconducting gap are smaller if the ferromagnets have a parallel spin orientation. Following this prediction, experiments have been performed, which have fully confirmed the model [2,3].

In a recent work, Mélin [4] has proposed a model in which the ferromagnets are metallic, and found a behavior opposite to the model by de Gennes [1]. It was found that the superconducting gap is larger if the ferromagnetic electrodes have a parallel spin orientation. It was also pointed out in Ref. [4] that non local superconducting correlations can be characterized by non local Gorkov functions and it was shown that the qualitative physics can be captured by simple wave functions involving linear superpositions of pair states [4].

Therefore, we have been proposed two antagonist points of view:

- (i) The work by de Gennes [1] is concerned with *insulating ferromagnets*. In these systems, there exists an effective ferromagnetic exchange field coupled to single electron states in the superconductor, that can be described first order perturbation theory. The focus in this description is put on single electron states.
- (ii) The recent work in Ref. [4] is focussed on non local pair correlations induced in *metallic ferromagnetic electrodes*. The electrons in different ferromagnetic electrodes are coupled by an effective antiferromagnetic exchange. The focus in this description is put on pair states.

The first question to be asked is: *Why should the de Gennes approach break-down with metallic ferromagnets ?* The answer is the following: when an electron with energy E penetrates a *metallic ferromagnet*, it couples to the

*melin@polycnrs-gre.fr

[†]U.P.R. 5001 du CNRS, Laboratoire conventionné avec l’Université Joseph Fourier

exchange field and acquires a spin energy. But the total energy is conserved. As a consequence a spin-up electron accelerates and a spin-down electron decelerates according to the following formula:

$$E = \frac{\hbar^2 k^2}{2m} = \frac{\hbar^2 (k^\sigma)^2}{2m} - h_{\text{ex}} S^z,$$

where h_{ex} is the exchange field in the ferromagnet, k is the longitudinal wave vector in the non magnetic region and k^σ is the longitudinal wave vector of spin- σ electrons in the ferromagnet. As a consequence we cannot treat $-h_{\text{ex}} S^z$ as a perturbation without ignoring the orbital degrees of freedom which is why we cannot apply the same perturbation theory as for insulating ferromagnets.

The second question to be asked is: *What is the physics associated to metallic ferromagnets?* The evidence that pair correlations play a central role with metallic ferromagnets can be seen from the calculation of the non local Gorkov functions (see Ref. [4]). From these Gorkov functions we deduce that spin-up and spin-down electrons in different ferromagnets are coupled by an effective *antiferromagnetic* exchange:

$$J = \Delta \left(\frac{a_0}{d_S} \right) \exp(-d_s/\xi_0), \quad (1)$$

where a_0 is the lattice spacing, d_S is the thickness of the superconducting layer and ξ_0 the BCS coherence length. Now we can follow the approach by de Jong and Beenakker [5] and count how many conduction channels are coupled by the effective exchange (1). We denote by N^\uparrow and N^\downarrow the number of spin-up and spin-down conduction channels in a spin-up ferromagnet. The total energy due to the exchange (1) is lower in the antiparallel alignment:

$$E_{\uparrow,\downarrow} - E_{\uparrow,\uparrow} = -(N^\uparrow - N^\downarrow) \Delta \left(\frac{a_0}{d_S} \right) \exp(-d_s/\xi_0).$$

The third question that should be asked is: *What is the consequence regarding the superconducting order parameter?* For insulating ferromagnets, the effective exchange field in the superconductor is a pair breaking perturbation. As a consequence the gap is smaller in the parallel alignment [1]. In the case of metallic ferromagnets, we obtain $\Delta_{\text{AF}} < \Delta_{\text{F}}$ while de Gennes has obtained $\Delta_{\text{AF}} > \Delta_{\text{F}}$ with insulating ferromagnets.

This article is devoted to solve microscopic models to demonstrate the validity of this picture. The model is given in section II, as well as technical preliminaries. We propose in section III a “gap kernel” approach and we find that the gap is smaller in the antiparallel alignment, in agreement with the physical picture given above. With this gap kernel approach we can also solve the model with insulating ferromagnets and find a behavior in agreement with the perturbative approach by de Gennes. We show that the physics in this problem can be understood by analyzing the lowest order Feynman diagrams. We perform exact diagonalizations in section IV which confirm the result of the gap kernel approach. Following the arguments given above, we propose in section V that our result for the self consistent order parameter ($\Delta_{\text{AF}} < \Delta_{\text{F}}$) is related to pair correlations among ferromagnetic electrodes that constitute a generalized proximity effect. We discuss in detail the matrices of Gorkov functions involved in the non local proximity effect.

II. TECHNICAL PRELIMINARIES

A. The model

We will consider in this work a superconductor in contact with several ferromagnetic electrodes. The superconductor is supposed to be three dimensional but we will use also a one dimensional geometry in the numerical simulations. We describe the superconductor by a tight binding BCS model in which the electrons can hop between neighboring “sites” on a square lattice having a lattice parameter a_0 . The BCS Hamiltonian takes the form

$$\mathcal{H} = \sum_{\langle \alpha, \beta \rangle, \sigma} -t \left(c_{\alpha,\sigma}^+ c_{\beta,\sigma} + c_{\beta,\sigma}^+ c_{\alpha,\sigma} \right) + \sum_{\alpha} \left(\Delta_{\alpha} c_{\alpha,\uparrow}^+ c_{\alpha,\downarrow}^+ + \Delta_{\alpha}^* c_{\alpha,\downarrow} c_{\alpha,\uparrow} \right), \quad (2)$$

where the summation in the kinetic term is carried out over neighboring pairs of sites. Without loss of generality, we assume that the superconductor conduction band is half-filled with therefore $k_F = \frac{\pi}{2a_0}$. Noting ϵ_F the Fermi energy, we have $\epsilon_F = t$. We can also use the notation $D = t$ for the band width. Since the physics should not depend on the

details of the band structure, we will use also a free electron dispersion relation $\epsilon(k) = \frac{\hbar^2 k^2}{2m}$, with $\epsilon_F = \frac{\hbar^2 k_F^2}{2m}$ the Fermi energy. This dispersion relation is truncated by a high energy cut-off $\epsilon(k_{\max}) = 2D = 2\epsilon_F$. The Hamiltonian (2) does not contain a coupling to electromagnetism. As a consequence the model cannot be used to describe orbital depairing but we know that orbital depairing is small for type-II superconductors such as Aluminum in a thin film geometry, and with the spin orientation of the ferromagnets parallel to the superconducting film [6,7].

B. The method

We will use a Green's function formalism (see for instance [8–12]) to solve the microscopic model defined in section II A. The first step involved in the calculation is to obtain the expression of the advanced and retarded propagators of the connected system $\hat{G}_{i,j}^{A,R}$ in terms of the advanced and retarded propagators of the disconnected system $\hat{g}_{i,j}^{A,R}$. The general form of the Dyson equation reads

$$\hat{G}^{R,A} = \hat{g}^{R,A} + \hat{g}^{R,A} \otimes \hat{\Sigma} \otimes \hat{G}^{R,A}, \quad (3)$$

where $\hat{\Sigma}$ is a self energy that contains all couplings of the tunnel Hamiltonian. The Green's functions of the connected system will also be called “renormalized Green's functions” because they incorporate all excursions of the electrons in the ferromagnetic electrodes. The convolution in (3) includes a summation over space labels and a convolution of times variables. Since we consider a stationary situation, the latter can be transformed into a product by Fourier transform.

The advanced Green's function takes the following form in the Nambu representation:

$$\hat{g}_{\alpha,\beta}^A(t, t') = -i\theta(t - t') \begin{pmatrix} \langle \{c_{\alpha,\uparrow}(t), c_{\beta,\uparrow}^+(t')\} \rangle & \langle \{c_{\alpha,\uparrow}(t), c_{\beta,\downarrow}(t')\} \rangle \\ \langle \{c_{\alpha,\downarrow}^+(t), c_{\beta,\uparrow}^+(t')\} \rangle & \langle \{c_{\alpha,\downarrow}^+(t), c_{\beta,\downarrow}(t')\} \rangle \end{pmatrix}, \quad (4)$$

where α and β are two arbitrary sites in the superconductor. A similar expression holds for the retarded Green's function. We will adopt the following notation for the Nambu components:

$$\hat{g}_{\alpha,\beta}^{A,R}(\omega) = \begin{pmatrix} g_{\alpha,\beta}^{A,R}(\omega) & f_{\alpha,\beta}^{A,R}(\omega) \\ f_{\alpha,\beta}^{A,R}(\omega) & g_{\alpha,\beta}^{A,R}(\omega) \end{pmatrix}.$$

The Nambu representation of the density of states $\hat{\rho}_{\alpha,\beta}(\omega) = \frac{1}{2i\pi} [\hat{g}_{\alpha,\beta}^A(\omega) - \hat{g}_{\alpha,\beta}^R(\omega)]$ will be noted

$$\hat{\rho}_{\alpha,\beta}(\omega) = \begin{pmatrix} \rho_g^{\alpha,\beta}(\omega) & \rho_f^{\alpha,\beta}(\omega) \\ \rho_f^{\alpha,\beta}(\omega) & \rho_g^{\alpha,\beta}(\omega) \end{pmatrix},$$

where $\rho_g^{\alpha,\beta}(\omega) = \frac{1}{2i\pi} [g_{\alpha,\beta}^A(\omega) - g_{\alpha,\beta}^R(\omega)]$ and $\rho_f^{\alpha,\beta}(\omega) = \frac{1}{2i\pi} [g_{\alpha,\beta}^A(\omega) - g_{\alpha,\beta}^R(\omega)]$. Once the renormalized advanced and retarded Green's functions has been evaluated using (3), we can evaluate the Keldysh component [8]

$$\hat{G}^{+,-} = [\hat{I} + \hat{G}^R \otimes \hat{\Sigma}] \otimes \hat{g}^{+,-} \otimes [\hat{I} + \hat{\Sigma} \otimes \hat{G}^A], \quad (5)$$

where $\hat{g}_{i,j}^{+,-} = 2i\pi n_F(\omega - \mu_{i,j})\hat{\rho}_{i,j}$. The Green's function given by (5) can be used either to calculate transport properties (see for instance [9] for the microscopic theory of the metal – insulator – metal junction) or to determine the self consistent value of the superconducting order parameter (see for instance [11] for the microscopic theory of the Josephson constriction). All information about non local superconducting correlations between two arbitrary sites α and β is contained in the Gorkov function $[G_{\alpha,\beta}^{+,-}(\omega)]_{1,2}$. We can thus use the Gorkov function to describe the proximity effect in a *non local* situation (see section V and Ref. [4]). The Gorkov function can be used to determine the self consistent value of the superconducting order parameter at any site β in the superconductor (see [7,11]):

$$\Delta_\beta = -U \int \frac{d\omega}{2i\pi} G_{\beta,\beta}^{+,-,1,2}(\omega), \quad (6)$$

where U is the microscopic attractive interaction.

In the following we will concentrate on equilibrium properties. Namely, the chemical potentials are identical in all electrodes and there is thus no current flow. In this situation the Keldysh Green's function (5) simplifies into

$$\hat{G}_{\text{eq}}^{+,-} = n_F(\omega - \mu_0) \left(\hat{G}^A - \hat{G}^R \right), \quad (7)$$

where μ_0 is the chemical potential. The calculations based on (7) will be presented in the main body of the article. In Appendix A we will rederive some of our results using Eq. (5). The calculation based on (5) turn out to be more complicated than the calculation based on (7). However, Eq. (5) is more general since it constitutes the starting point to calculate the self consistent superconducting order parameter in an out-of-equilibrium situation. (an issue that we keep for a future publication).

Self consistency can be obtained by iterating the process on Fig. 1 which starts with a uniform gap profile $[\Delta_\beta]$. From this gap profile we calculate the Green's functions $g_{\alpha,\beta}(\omega)$ of the superconductor isolated from the ferromagnetic electrodes. From Eqs. (3) or (7), we obtain the renormalized Green's function $G_{\alpha,\beta}^{A,R}$. From the Dyson-Keldysh equation (5) we deduce the Gorkov function $[G_{\alpha,\alpha}^{+,-}(\omega)]_{1,2}$, which is used to recalculate the superconducting order parameter profile via the self consistency equation (6).

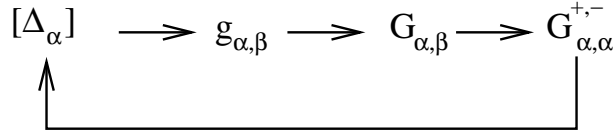


FIG. 1. Representation of the successive operations involved in the calculation of the self consistent value of the superconducting order parameter.

C. The different approaches used to determine the self consistent gap profile

1. Position of the problem

Our problem is to find reliable determinations of the self consistent order parameter. It is in practice impossible to make an exact analytical calculation of the self consistent order parameter except in the limit already considered in Ref. [4] where the superconducting gap is uniform in space (the superconductor is smaller than the coherence length). The reason why we cannot find exact solutions is the following. Let us start with a uniform gap profile $\Delta_\beta \equiv \Delta_0$ and consider the successive operations on Fig. 1. Because of the contacts between the superconductor and the ferromagnetic electrodes, the renormalized Green's functions are not translational invariant. As a result in the next iteration, the superconducting order parameter is not translational invariant. The expression of the Green's functions of an isolated superconductor in the presence of a non uniform superconducting order parameter is not known in general. The self consistency relation (6) thus becomes a functional equation:

$$\Delta_\beta = -U \int \frac{d\omega}{2i\pi} G_{\beta,\beta}^{+,-,1,2}([\Delta], \omega), \quad (8)$$

where the notation $[\Delta]$ means that the right hand side depends on all values of the gap profile. As a consequence, we cannot find exact solutions for the gap profile.

2. Local and pseudo-local approaches

We present in section III an approximate analytical treatment in which the *functional* self consistency equation (8) is replaced by a *local* equation:

$$\Delta_\beta = -U \int \frac{d\omega}{2i\pi} G_{\beta,\beta}^{+,-,1,2}(\Delta_\beta, \omega). \quad (9)$$

To transform (8) into (9), we assume that the Green's functions of the isolated superconductor in the presence of a non uniform gap has the same energy dependence as the Green's function with a uniform gap. With this assumption the Green's function depends on an unknown parameter which we call the gap kernel. We will discuss several choices of the gap kernel. We first show in section III that the gap profile can be obtained analytically if one assumes a local gap kernel. A model with the simplest non local gap kernel is solved numerically in section III D.

3. Exact diagonalizations

We present in section IV another approach in which we use exact diagonalizations to solve exactly the functional form of the self consistency equation (8). This numerical method is restricted to small system sizes. We will find that the exact diagonalizations are consistent with the gap kernel approaches in the sense that we find $\Delta_{\text{AF}} < \Delta_{\text{F}}$ with both approaches.

D. Green's functions in the presence of a uniform superconducting order parameter

We end-up this preliminary section with a few remarks on the Green's functions of a superconductor having a uniform superconducting order parameter: $\Delta_{\beta} \equiv \Delta_0$ for all sites β .

1. Spectral representation

With a superconducting uniform gap, the spectral representation can be evaluated explicitly:

$$g_{\alpha,\beta}^A(\omega) = \frac{1}{\mathcal{N}} \sum_{\vec{k}} e^{i\vec{k} \cdot (\vec{x}_{\alpha} - \vec{x}_{\beta})} \left[\frac{|u_k|^2}{\omega - (\mu_S + E_k) - i\eta} + \frac{|v_k|^2}{\omega - (\mu_S - E_k) - i\eta} \right] \quad (10)$$

$$f_{\alpha,\beta}^A(\omega) = \frac{1}{\mathcal{N}} \sum_{\vec{k}} e^{i\vec{k} \cdot (\vec{x}_{\alpha} - \vec{x}_{\beta})} u_k^* v_k \left[-\frac{1}{\omega - (\mu_S + E_k) - i\eta} + \frac{1}{\omega - (\mu_S - E_k) - i\eta} \right], \quad (11)$$

where \mathcal{N} is the number of sites. $E_k = \sqrt{\Delta_0^2 + (\xi_k)^2}$ is the energy of the quasiparticle, $\xi_k = \epsilon_k - \mu$ is the kinetic energy, and $(u_k)^2 = \frac{1}{2} \left(1 + \frac{\xi_k}{E_k} \right)$, $(v_k)^2 = \frac{1}{2} \left(1 - \frac{\xi_k}{E_k} \right)$ are the BCS coherence factors.

2. Green's function below the superconducting gap

Integrating (10) and (11) over wave vector and assuming $\omega < \Delta$, we obtain

$$\begin{aligned} \hat{g}_{\alpha,\beta}^{R,A}(\omega) &= \frac{ma_0^3}{\hbar^2} \frac{1}{2\pi|\vec{x}_{\alpha} - \vec{x}_{\beta}|} \exp\left(-\frac{|\vec{x}_{\alpha} - \vec{x}_{\beta}|}{2\xi(\omega)}\right) \\ &\times \left\{ \frac{\sin \varphi}{\sqrt{\Delta_0^2 - (\omega - \mu_S)^2}} \begin{bmatrix} -(\omega - \mu_S) & \Delta_0 \\ \Delta_0 & -(\omega - \mu_S) \end{bmatrix} - \cos \varphi \begin{bmatrix} 1 & 0 \\ 0 & 1 \end{bmatrix} \right\}, \end{aligned} \quad (12)$$

where the superconductor coherence length is given by

$$\xi(\omega) = \xi_0 \frac{\Delta_0}{\sqrt{\Delta_0^2 - (\omega - \mu_S)^2}} \quad (13)$$

with

$$\xi_0 = \frac{\epsilon_F}{k_F \Delta_0} \quad (14)$$

the BCS coherence length. The electronic phase appearing in (16) is given by

$$\varphi = k_F |\vec{x}_{\alpha} - \vec{x}_{\beta}|. \quad (15)$$

3. Green's function above the superconducting gap

Integrating (10) and (11) over wave vector and assuming $\omega > \Delta$, we obtain

$$\begin{aligned}\hat{g}_{\alpha,\beta}^{R,A}(\omega) &= \frac{ma_0^3}{\hbar^2} \frac{1}{2\pi|\vec{x}_\alpha - \vec{x}_\beta|} \exp[\mp i\psi(\omega)] \\ &\times \left\{ \frac{\mp i \sin \varphi}{\sqrt{(\omega - \mu_S)^2 - \Delta_0^2}} \begin{bmatrix} -(\omega - \mu_S) & \Delta_0 \\ \Delta_0 & -(\omega - \mu_S) \end{bmatrix} - \cos \varphi \begin{bmatrix} 1 & 0 \\ 0 & 1 \end{bmatrix} \right\},\end{aligned}\quad (16)$$

where the phase in the prefactor is given by

$$\psi(\omega) = \frac{1}{v_F} |\vec{x}_\alpha - \vec{x}_\beta| \sqrt{(\omega - \mu_S)^2 - \Delta_0^2}. \quad (17)$$

We note that if $\omega \gg \Delta$, the Green's function reduces to

$$g_{\alpha,\beta}^A(\omega) = -\frac{ma_0^3}{\hbar^2} \frac{1}{2\pi R_{\alpha,\beta}} \exp[i(\psi(\omega) + \varphi(\omega))],$$

which will be used in section III G.

4. Determination of the superconducting order parameter in the BCS model

In the case of an isolated superconductor, the self consistency equation (6) becomes

$$\Delta_0 = -U \int_0^D \frac{d\omega}{2i\pi} g_{\text{loc}}^{+,-,1,2}(\omega), \quad (18)$$

where D is the electronic bandwidth and $g_{\text{loc}}^{+,-,1,2} = 2i\pi n_F(\omega - \mu_S)\rho_f^{\text{loc}}$ is the local anomalous propagator (see section II B). The local anomalous propagator (16) is diverging if α and β correspond to the same site. To regularize local quantities, we replace $\vec{x}_\alpha = \vec{x}_\beta$ by $|\vec{x}_\alpha - \vec{x}_\beta| = a_0$ in which case the local propagator is a finite quantity, having the dimension of the inverse of an energy.

To evaluate (18) we calculate only the asymptotic high energy behavior of the Gorkov function because the integral over energy in (18) diverges logarithmically at high energy. We deduce from (18) the BCS relation for the superconducting order parameter (see for instance [7]):

$$\Delta_0 = D \left[\cosh \left(\frac{1}{U} \frac{2\pi^2 \hbar^2}{ma_0^2} \right) \right]^{-1} \simeq 2D \exp \left(-\frac{1}{U} \frac{2\pi^2 \hbar^2}{ma_0^2} \right), \quad (19)$$

which is exponentially small in $1/U$.

5. Determination of the superconducting order parameter in the presence of Pauli paramagnetism

Let us now include Pauli paramagnetism [6,13–15] in the BCS model under the form of a spin energy term $-h_0 \sum_{\vec{k}} [c_{\vec{k},\uparrow}^\dagger c_{\vec{k},\uparrow} - c_{\vec{k},\downarrow}^\dagger c_{\vec{k},\downarrow}]$. This problem is already very close to the insulating F/S/F heterostructure in which there is an effective exchange field induced in the superconductor [1]. The Bogoliubov-de Gennes equations (see [16]) in the presence of the spin energy term take the form

$$(E + h_0) \begin{bmatrix} u_\uparrow(x) \\ v_\downarrow(x) \end{bmatrix} = \begin{bmatrix} \mathcal{H}_e - \mu & \Delta_0 \\ \Delta_0 & -(\mathcal{H}_e^* - \mu) \end{bmatrix} \begin{bmatrix} u_\uparrow(x) \\ v_\downarrow(x) \end{bmatrix}, \quad (20)$$

where \mathcal{H}_e is the kinetic energy. We deduce from (20) the energy of spin-up quasiparticles:

$$E_k = -h_0 + \sqrt{(\epsilon_k - \mu)^2 + \Delta^2}.$$

The coherence factors have been already given in Ref. [17]:

$$(u_\uparrow)^2 = 1 - (v_\downarrow)^2 = \frac{1}{2} \left(1 + \frac{\sqrt{(E + h_0)^2 - \Delta^2}}{E + h_0} \right),$$

and similar expressions can be obtained for spin-down quasiparticles. The anomalous propagator generalizing (12) takes the form

$$f_{\alpha,\beta}^{R,A}(\omega) = \frac{ma_0^3}{\hbar^2} \frac{1}{2\pi|\vec{x}_\alpha - \vec{x}_\beta|} \exp\left(-\frac{|\vec{x}_\alpha - \vec{x}_\beta|}{2\xi(\omega)}\right) \frac{\sin \varphi}{\sqrt{\Delta_0^2 - (\omega - \mu_S)^2}} \quad (21)$$

$$\times \frac{\Delta_0}{2} \left[\frac{1}{\sqrt{\Delta_0^2 - (\omega + h_0)^2}} + \frac{1}{\sqrt{\Delta_0^2 - (\omega - h_0)^2}} \right]. \quad (22)$$

The self consistency equation (18) leads to

$$\Delta_0 = 2D \exp \left[-\frac{1}{U} \frac{2\pi^2 \hbar^2}{ma_0^2} - \left(\frac{h_0}{D} \right)^2 \right],$$

where we assumed that the exchange field is small compared to the bandwidth of the superconductor ($h_0 \ll D$). The spin energy term reduces the superconducting gap, as it is expected for a pair breaking perturbation [18,19].

III. SELF CONSISTENT EVALUATION OF THE SUPERCONDUCTING ORDER PARAMETER: GAP KERNEL APPROACHES

The self consistency equation for the superconducting order parameter (8) is a functional of the gap profile. In this section, we replace the functional equation (8) by the local equation (9) or by a pseudo-local equation. More precisely, it is assumed that the Green's functions $g_{\alpha,\beta}$ and $g_{\alpha',\beta}$ of the disconnected superconductor in the presence of an inhomogeneous superconducting order parameter have the same energy dependence as (16). The remaining free parameter in (16) is the value of the superconducting order parameter Δ_0 . The value of Δ_0 is *a priori* a functional of the gap profile: $\Delta_0 = \Delta_0[\Delta]$. We refer to this functional as the “gap kernel”. In sections III A, III B and III C it is assumed that the gap kernel entering the Green's functions $g_{\alpha,\beta}$ and $g_{\alpha',\beta}$ is purely local: $\Delta_0[\Delta] = \Delta_\beta$. With this choice of the gap kernel we can obtain analytic expressions for the self consistent order parameter. The disadvantage is that this choice of the gap kernel Δ_0 introduces an unphysical constraint. Namely, the propagators $g^{\alpha,\beta}$ and $f^{\alpha,\beta}$ are no more symmetric in the exchange of sites α and β : $g^{\alpha,\beta} \neq g^{\beta,\alpha}$ and $f^{\alpha,\beta} \neq f^{\beta,\alpha}$. To solve this inconsistency, we consider in section III D another possibility for the gap kernel: $\Delta_0 = \sqrt{\Delta_\alpha \Delta_\beta}$. With this pseudo-local gap kernel, the propagators $g^{\alpha,\beta}$ and $f^{\alpha,\beta}$ are symmetric in the exchange of sites α and β but we cannot find analytical solutions anymore.

A. Gap profile: (I) Single-channel problem with fixed electronic phases

Let us now implement the local gap kernel approach in the case of the single channel problem corresponding to Fig. 2. We first make the additional assumption that the electronic phase in the Green's function (16) does not depend on distance: $\varphi = -\pi/2$ for all distances. The role of phase averaging will be discussed in section III G.

Using the Dyson equation for the propagator (3) and the expression (7) of the equilibrium Gorkov function, we obtain easily the local Gorkov function

$$G_{\beta,\beta}^{+,-} = 2i\pi n_F(\omega) \left\{ \rho_f^{\beta,\beta} + \frac{|t_{a,\alpha}|^2}{2i\pi} \left[\frac{1}{\mathcal{D}^A} g_{1,1}^{a,a,A} g_{\beta,\alpha,A}^{a,a,A} f_{\alpha,\beta,A}^{a,a,A} - \frac{1}{\mathcal{D}^R} g_{1,1}^{a,a,R} g_{\beta,\alpha,R}^{a,a,R} f_{\alpha,\beta,R}^{a,a,R} \right] \right\}, \quad (23)$$

with

$$\mathcal{D} = 1 - |t^{a,\alpha}|^2 g_{1,1}^{a,a} g_{\alpha,\alpha}^{a,a}. \quad (24)$$

We deduce the gap profile in the local gap kernel approach:

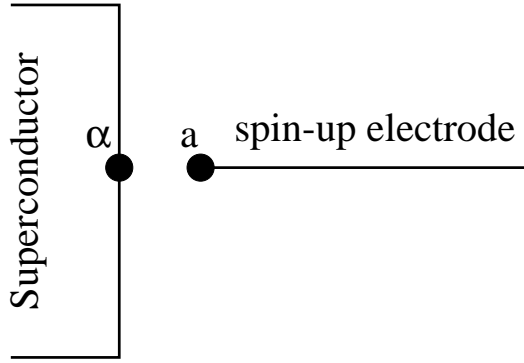


FIG. 2. Representation of a model in which a single channel spin-up electrode is in contact with a superconductor.

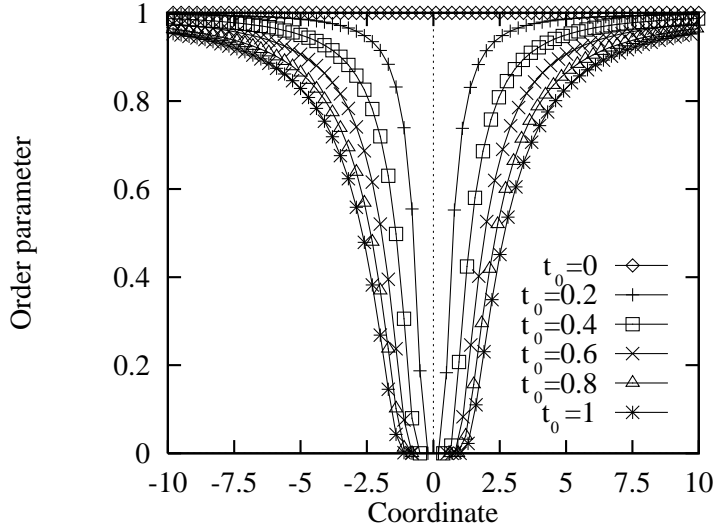


FIG. 3. Variation of the superconducting order parameter with a single ferromagnetic channel and with a local gap kernel: $\Delta_0[\Delta] = \Delta_\beta$. We used realistic parameters: the Fermi energy is $\epsilon_F = 10$ eV and the value of the attractive electron – electron interaction is such that the bulk superconducting order parameter is $\Delta_{\text{bulk}} = 1$ meV.

$$\Delta_\beta = 2D \exp \left\{ -\frac{1}{U} \frac{2\pi^2 \hbar^2}{ma_0^2} \left[1 - \left(\frac{a_0}{R_{\alpha,\beta}} \right)^2 \frac{t_0^2}{1+t_0^2} \right]^{-1} \right\}, \quad (25)$$

where

$$t_0 = \frac{t}{\epsilon_F} \frac{(a_0 k_F)^2}{4\pi} \quad (26)$$

is the hopping energy normalized to the Fermi energy. $R_{\alpha,\beta} = |\vec{x}_\alpha - \vec{x}_\beta|$ is the distance between sites α and β in the superconductor. The superconducting order parameter is minimum close to the contact with the ferromagnetic channel. The minimum value of the superconducting order parameter is obtained from Eq. (25) by replacing $R_{\alpha,\beta}$ by the lattice spacing a_0 :

$$\Delta_\alpha = 2D \exp \left\{ -\frac{1}{U} \frac{2\pi^2 \hbar^2}{ma_0^2} [1 + t_0^2] \right\}.$$

Far away from the contact, the superconducting order parameter tends to the bulk value given by Eq. (19). The complete gap profile is shown on Fig. 3 for several values of the hopping between the superconductor and the ferromagnetic channel.

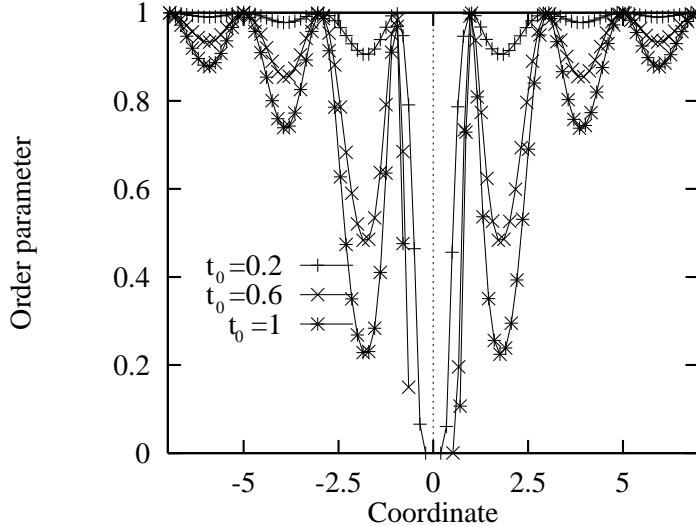


FIG. 4. Variation of the superconducting order parameter as a function of the distance to the contact with a single ferromagnetic channel and with a local gap kernel: $\Delta_0[\Delta] = \Delta_\beta$. We incorporated the oscillatory phase factor in (27) and suppose that $k_F a = \frac{\pi}{2a_0}$. The period of the oscillations is therefore $2a_0$. The parameters are the same as on Fig. 3.

B. Gap profile: (II) Role of $2k_F$ oscillations in the single-channel problem

Now we discuss the role played by the phase φ appearing in the Green's function $g_{\alpha,\beta}$ (see Eq.(16)). In the presence of this phase factor, the self consistent superconducting order parameter develops $2k_F$ oscillations:

$$\Delta_\beta = 2D \exp \left\{ -\frac{1}{U} \frac{2\pi^2 \hbar^2}{ma_0^2} \left[1 - \left(\frac{a_0}{R_{\alpha,\beta}} \right)^2 \frac{t_0^2}{1+t_0^2} \sin^2(k_F R_{\alpha,\beta}) \right]^{-1} \right\}, \quad (27)$$

where $R_{\alpha,\beta} = |\vec{x}_\alpha - \vec{x}_\beta|$. The gap profile is shown on Fig. 4. One may notice that $\Delta_{\text{bulk}} - \Delta(R_{\alpha,\beta})$ deduced from Fig. 4 is related to the wave function of a spin-up electron injected at site α in the superconductor. Namely the superconducting gap is maximal when the spin-up wave function is minimal.

C. Gap profile and gap difference function: (III) Two-channel problem with fixed electronic phases

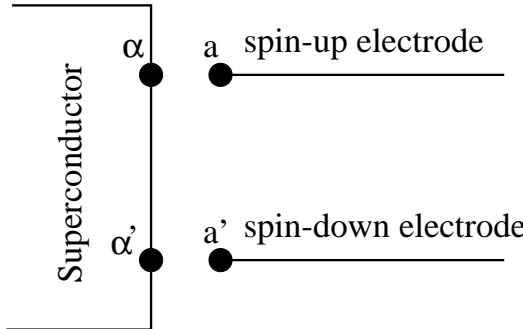


FIG. 5. Representation of a model in which two single channel spin-up and spin-down electrodes are in contact with a superconductor.

Let us now apply the local approach to the two-channel model on Fig. 5 and calculate the self consistent superconducting order parameter. We assume that the electronic phases are fixed to the value $\varphi = -\pi/2$ for all distances.

1. Antiferromagnetic alignment

Let us consider the model on Fig. 5 in which two single-channel spin-up and spin-down electrodes are in contact with a superconductor. The local Green's function takes the form

$$\hat{G}^{\beta,\beta} = \hat{g}^{\beta,\beta} + \hat{g}^{\beta,\alpha} \hat{t}^{\alpha,a} \hat{G}^{a,\beta} + \hat{g}^{\beta,\alpha'} \hat{t}^{\alpha',a'} \hat{G}^{a',\beta}. \quad (28)$$

Therefore, we need to evaluate the following propagators:

$$\hat{G}^{a,\beta} = t^{a,\alpha} g_{1,1}^{a,a} \begin{bmatrix} \tilde{g}^{\alpha,\beta} & \tilde{f}^{\alpha,\beta} \\ 0 & 0 \end{bmatrix} \quad (29)$$

$$\hat{G}^{a',\beta} = -t^{a',\alpha'} g_{2,2}^{a',a'} \begin{bmatrix} 0 & 0 \\ \tilde{f}^{\alpha',\beta} & \tilde{g}^{\alpha',\beta} \end{bmatrix} \quad (30)$$

$$\cdot \quad (31)$$

The renormalized propagators \tilde{f} 's and \tilde{g} 's are given by

$$\tilde{g}^{\alpha,\beta} = \frac{1}{\mathcal{D}_{\text{AF}}} \left[g^{\alpha,\beta} + |t^{a',\alpha'}|^2 g_{2,2}^{a',a'} \left(f^{\alpha,\alpha'} f^{\alpha',\beta} - g^{\alpha',\alpha'} g^{\alpha,\beta} \right) \right] \quad (32)$$

$$\tilde{f}^{\alpha,\beta} = \frac{1}{\mathcal{D}_{\text{AF}}} \left[f^{\alpha,\beta} + |t^{a',\alpha'}|^2 g_{2,2}^{a',a'} \left(f^{\alpha,\alpha'} g^{\alpha',\beta} - g^{\alpha',\alpha'} f^{\alpha,\beta} \right) \right], \quad (33)$$

with

$$\mathcal{D}_{\text{AF}} = \left[1 - |t^{a,\alpha}|^2 g_{1,1}^{a,a} g^{\alpha,\alpha} \right] \left[1 - |t^{a',\alpha'}|^2 g_{2,2}^{a',a'} g^{\alpha',\alpha'} \right] - |t^{a,\alpha}|^2 |t^{a',\alpha'}|^2 g_{1,1}^{a,a} g_{2,2}^{a',a'} f^{\alpha,\alpha'} f^{\alpha',\alpha}. \quad (34)$$

To obtain the self consistent superconducting order parameter, we should evaluate the high energy behavior of the Green's functions appearing in the local Gorkov function (7). \mathcal{D}_{AF} given by (34) reduces to

$$\mathcal{D}_{\text{AF}} \simeq \left[1 - |t^{a,\alpha}|^2 g_{1,1}^{a,a} g^{\alpha,\alpha} \right] \left[1 - |t^{a',\alpha'}|^2 g_{2,2}^{a',a'} g^{\alpha',\alpha'} \right]$$

at high energy, where we discarded a term of order $1/\omega^2$. It is also useful to calculate the high energy behavior of the following Green's functions:

$$\tilde{f}^{\alpha,\beta,A} \simeq i \frac{1}{\mathcal{D}_{\text{AF}}} \frac{\Delta}{\omega} \frac{a_0}{R_{\alpha,\beta}} \left\{ 1 - |t_0^{a',\alpha'}|^2 \left[\frac{a_0 R_{\alpha,\beta}}{R_{\alpha,\alpha'} R_{\alpha',\beta}} - 1 \right] \right\} \quad (35)$$

$$\tilde{g}^{\alpha',\beta,A} \simeq i \frac{1}{\mathcal{D}_{\text{AF}}} \frac{a_0}{R_{\alpha',\beta}} (1 + |t_0^{a,\alpha}|^2). \quad (36)$$

Using these relations, we obtain the asymptotic high-energy form of the local Gorkov function (7):

$$\hat{G}_{\beta,\beta}^{+,-} = -2i\pi n_F(\omega) \frac{ma_0^2}{2\pi^2 \hbar^2} \left(\frac{\Delta}{\omega} \right) \Lambda_{\text{Metal}}^{\text{AF}}, \quad (37)$$

with

$$\Lambda_{\text{Metal}}^{\text{AF}} = 1 - \frac{a_0^2}{R_{\alpha,\beta}^2} \left(\frac{|t_0^{a,\alpha}|^2}{1 + |t_0^{a,\alpha}|^2} \right) - \frac{a_0^2}{R_{\alpha',\beta}^2} \left(\frac{|t_0^{a',\alpha'}|^2}{1 + |t_0^{a',\alpha'}|^2} \right) + \frac{a_0^3}{R_{\alpha,\beta} R_{\alpha',\beta} R_{\alpha,\alpha'}} \left(\frac{|t_0^{a,\alpha}|^2}{1 + |t_0^{a,\alpha}|^2} \right) \left(\frac{|t_0^{a',\alpha'}|^2}{1 + |t_0^{a',\alpha'}|^2} \right), \quad (38)$$

where $t_0^{a,\alpha}$ and $t_0^{a',\alpha'}$ are the tunnel matrix elements normalized to the Fermi energy (see Eq. (26)).

2. Ferromagnetic alignment

Using the Gorkov function (7), we obtain

$$\hat{G}_{\beta,\beta}^{+,-} = -2i\pi n_F(\omega) \frac{ma_0^2}{2\pi^2 \hbar^2} \left(\frac{\Delta}{\omega} \right) \Lambda_{\text{Metal}}^{\text{F}} \quad (39)$$

at high energy, with

$$\Lambda_{\text{Metal}}^F = 1 - \frac{a_0^2}{R_{\alpha,\beta}^2} \left(\frac{|t_0^{a,\alpha}|^2}{1 + |t_0^{a,\alpha}|^2} \right) - \frac{a_0^2}{R_{\alpha',\beta}^2} \left(\frac{|t_0^{a',\alpha'}|^2}{1 + |t_0^{a',\alpha'}|^2} \right) + 2|t_0^{a,\alpha}|^2|t_0^{a',\alpha'}|^2 \frac{1}{\mathcal{D}_F} \frac{a_0^3}{R_{\alpha,\beta} R_{\alpha',\beta} R_{\alpha,\alpha'}}, \quad (40)$$

with

$$\mathcal{D}_F = [1 - |t^{a,\alpha}|^2 g_{1,1}^{a,a} g^{\alpha,\alpha}] [1 - |t^{a',\alpha'}|^2 g_{2,2}^{a',a'} g^{\alpha',\alpha'}] - |t^{a,\alpha}|^2 |t^{a',\alpha'}|^2 g_{1,1}^{a,a} g_{2,2}^{a',a'} g^{\alpha,\alpha'} g^{\alpha',\alpha}. \quad (41)$$

To order $1/R^3$, Eq. (40) becomes

$$\Lambda_{\text{Metal}}^F = 1 - \frac{a_0^2}{R_{\alpha,\beta}^2} \left(\frac{|t_0^{a,\alpha}|^2}{1 + |t_0^{a,\alpha}|^2} \right) - \frac{a_0^2}{R_{\alpha',\beta}^2} \left(\frac{|t_0^{a',\alpha'}|^2}{1 + |t_0^{a',\alpha'}|^2} \right) + 2 \frac{a_0^3}{R_{\alpha,\beta} R_{\alpha',\beta} R_{\alpha,\alpha'}} \left(\frac{|t_0^{a,\alpha}|^2}{1 + |t_0^{a,\alpha}|^2} \right) \left(\frac{|t_0^{a',\alpha'}|^2}{1 + |t_0^{a',\alpha'}|^2} \right). \quad (42)$$

Comparing Eqs. (38) and (42), we see that:

- (i) As expected, the “local” contributions of order $1/R_{\alpha,\beta}^2$ and $1/R_{\alpha',\beta}^2$ do not depend on the relative spin orientation of the ferromagnetic electrodes.
- (ii) The lowest order “non local” contribution arises at order $1/[R_{\alpha,\beta} R_{\alpha',\beta} R_{\alpha,\alpha'}]$, and depends on the relative spin orientation of the ferromagnetic electrodes via a factor of two in Eq. (42), not present in Eq. (38). This factor of two – as well as the sign of the non local contribution – can receive a simple interpretation which will be given in section III K.

3. Gap profiles

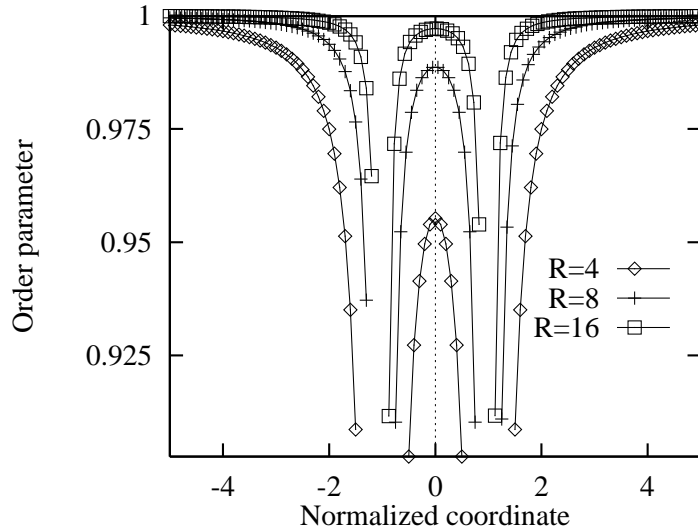


FIG. 6. Variation of the superconducting order parameter with a local gap kernel: $\Delta_0[\Delta] = \Delta_\beta$. It is assumed that the point β is aligned with the points α and α' . The coordinate is normalized to the separation $R_{\alpha,\alpha'}$ between the contacts. The different curves correspond to $R_{\alpha,\alpha'} = 4$ (\diamond), $R_{\alpha,\alpha'} = 8$ (+) and $R_{\alpha,\alpha'} = 16$ (\square). We used the same parameters as on Fig. 3. The contacts have a low transparency: $t_0^{a,\alpha} = t_0^{a',\alpha'} = 0.1$. The ferromagnetic electrodes have an antiparallel spin orientation.

The gap profiles are shown on Fig. 6 in the tunnel regime and Fig. 7 in the high transparency regime. The gap is reduced close to the contacts with the ferromagnets, which was already obtained for the single channel model in sections III A and III B (see Figs. 3 and 4).

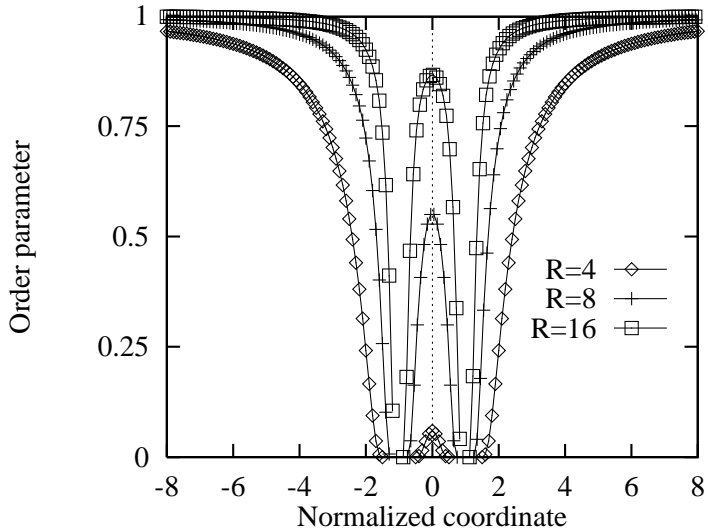


FIG. 7. The same as Fig. 7 with high transparency contacts: $t_0^{a,\alpha} = t_0^{a',\alpha'} = 1$.

4. Gap difference function

At each point β in the superconductor, we define the gap difference function as

$$\delta_\beta = 2 \frac{\Delta_\beta^F - \Delta_\beta^{AF}}{\Delta_\beta^F + \Delta_\beta^{AF}}. \quad (43)$$

The perturbative approach used by de Gennes for insulating ferromagnets leads to $\delta_\beta < 0$ [1]. We have shown on Fig. 8 the variation of the gap difference function deduced from (37) – (42) with metallic ferromagnets. We obtain $\delta_\beta > 0$. This is a first evidence showing that there is a new physics associated to metallic ferromagnets.

The gap difference function takes a simple form if the distance to the ferromagnetic electrodes is sufficiently large. In this case the gap difference function is found to be

$$\delta_\beta \simeq \frac{1}{U} \frac{2\pi^2 \hbar^2}{ma_0^2} \frac{|t_0^{a,\alpha}|^2}{1 + |t_0^{a,\alpha}|^2} \frac{|t_0^{a',\alpha'}|^2}{1 + |t_0^{a',\alpha'}|^2} \frac{a_0^3}{R_{\alpha,\beta} R_{\alpha',\beta} R_{\alpha,\alpha'}}. \quad (44)$$

We will comment on (44) in section III E.

D. Effect of a non local gap kernel

Now we improve the gap kernel method, and consider the simplest non local gap kernel for the Green's function $g^{\alpha,\beta}$: $\Delta_0[\Delta] = \sqrt{\Delta_\alpha \Delta_\beta}$. We consider the one dimensional geometry on Fig. 9 but we use the form (16) of the three dimensional Green's function. A numerical program is used to iterate the process on Fig. 1 and we use the asymptotic form of the Gorkov functions at high energy.

We first used realistic parameters: $\Delta_{\text{bulk}} = 1$ meV, $D = 10^4$ meV, with therefore $\Delta_{\text{bulk}}/D = 10^{-4}$. With these parameters, we find that $\delta_\beta > 0$, namely the ferromagnetic gap is larger than the antiferromagnetic gap (see Fig. 10).

We repeated the same calculation with the parameters that will be used in section IV for the exact diagonalizations: $\Delta_{\text{bulk}} = 0.2$, $D = 1$, with therefore $\Delta_{\text{bulk}}/D = 0.2$, far above the realistic value $\simeq 10^{-4}$. With these parameters, we also find that $\delta_\beta > 0$ (see Fig. 11).

From Figs. 10 and 11 we deduce that the gap function has the following scaling form at large distance:

$$\delta_\beta \propto \frac{1}{U} \frac{2\pi^2 \hbar^2}{ma_0^2} \frac{a_0}{|x_\alpha - x_{\alpha'}|} \frac{a_0}{|x_\beta - x_\alpha|} \frac{a_0}{|x_\beta - x_{\alpha'}|}, \quad (45)$$

which is identical to the scaling form (44) obtained with a local gap kernel.

We conclude that the model with the pseudo-local gap kernel $\Delta_0[\Delta] = \sqrt{\Delta_\alpha \Delta_\beta}$ behaves like the model with a local gap kernel $\Delta_0[\Delta] = \Delta_\beta$, which justifies *a posteriori* the investigation of the local gap kernel model.

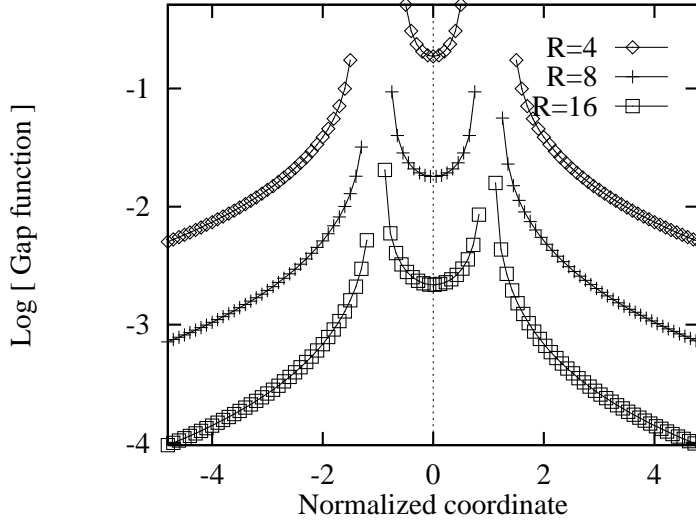


FIG. 8. Variation of the logarithm of the gap difference function (43) with a local gap kernel: $\Delta_0[\Delta] = \Delta_\beta$. The ferromagnetic gap is larger than the antiferromagnetic gap. The parameters are the same as on Fig. 3. The contacts have a high transparency: $t_0^{a,\alpha} = t_0^{a',\alpha'} = 1$.

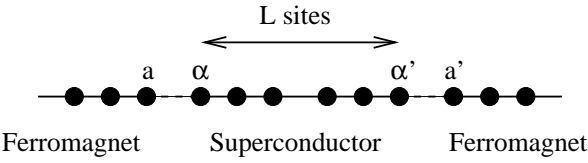


FIG. 9. The geometry treated in the numerical simulation. A superconductor on a one dimensional segment with L sites is connected to two ferromagnets.

E. Role of screening

We found that the gap difference function (43) takes a simple scaling form at large distance, both with a local gap kernel (see (44)) and with a non local gap kernel (see (45)). Eqs. (44) and (45) would suggest that there is no length scale associated to the screening of the ferromagnetic electrodes. This is not acceptable physically because we know that there should be additional exponential prefactors in (44) and (45):

$$\delta_\beta \propto \frac{1}{U} \frac{2\pi^2 \hbar^2}{ma_0^2} \frac{a_0}{|x_\alpha - x_{\alpha'}|} \exp\left(-\frac{|x_\alpha - x_{\alpha'}|}{\xi_0}\right) \frac{a_0}{|x_\beta - x_\alpha|} \exp\left(-\frac{|x_\beta - x_\alpha|}{\xi_0}\right) \frac{a_0}{|x_\beta - x_{\alpha'}|} \exp\left(-\frac{|x_\beta - x_{\alpha'}|}{\xi_0}\right), \quad (46)$$

where ξ_0 is the BCS coherence length given by (14). The fact that we have obtained (44) and (45) instead of (46) is in our opinion an artifact of the approximation used in the gap kernel approach.

F. Gap kernel approach to the F/S/F heterostructure with insulating ferromagnets

Let us now consider the problem originally considered by de Gennes [1] in which the ferromagnets are insulating. The propagator relevant to describe a ferromagnetic insulator decays exponentially with distance and is such that $g_{i,j}^A = g_{i,j}^R$. In particular the local propagators $g_{a,a}$ and $g_{a',a'}$ are real numbers. We implicitly assume that the bandwidth D of the superconductor is smaller than the charge gap of the ferromagnet. It is straightforward to modify the calculations presented in section III C to describe an insulating ferromagnet rather than a metallic ferromagnet. The Gorkov functions are still given by (37) and (39) but with a different form of Λ^{AF} and Λ^{F} . The expression of the Gorkov functions to order $1/R^3$ is the following:

$$\Lambda_{\text{Ins}}^{\text{AF}} = 1 - \frac{a_0^2}{R_{\alpha,\beta}^2} \left(\frac{|t_0^{a,\alpha}|^4}{1 + |t_0^{a,\alpha}|^4} \right) - \frac{a_0^2}{R_{\alpha',\beta}^2} \left(\frac{|t_0^{a',\alpha'}|^4}{1 + |t_0^{a',\alpha'}|^4} \right) \quad (47)$$

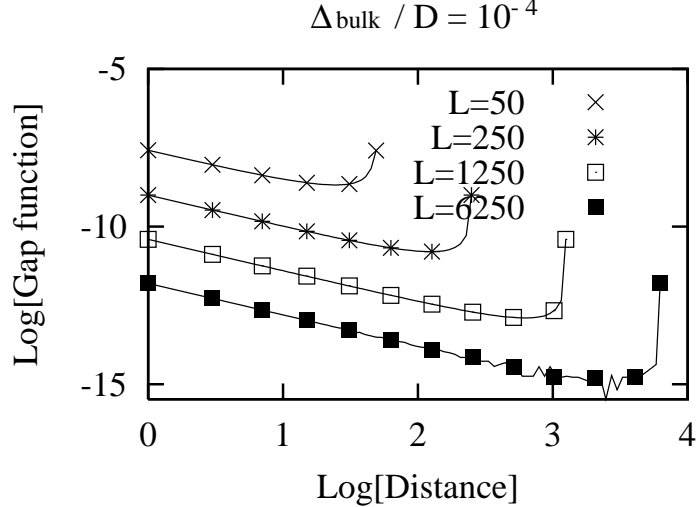


FIG. 10. Log-log plot of the variation of the gap difference function, with the geometry on Fig. 9, and with realistic parameters ($\Delta_{\text{bulk}} = 1$ meV, $D = 10$ meV), and $t_0^{a,\alpha} = t_0^{b,\beta} = 0.05$. We used a pseudo-local gap kernel: $\Delta_0[\Delta] = \sqrt{\Delta_\alpha \Delta_\beta}$. The ferromagnetic gap is larger than the antiferromagnetic gap. With these parameters the ratio between the superconducting gap and the bandwidth is $\Delta_{\text{bulk}}/D = 10^{-4}$.

$$\begin{aligned}
& -\frac{a_0^3}{R_{\alpha,\beta} R_{\alpha',\beta} R_{\alpha,\alpha'}} \left(1 - |t_0^{a,\alpha}|^2 |t_0^{a',\alpha'}|^2 \right) \left(\frac{|t_0^{a,\alpha}|^2}{1 + |t_0^{a,\alpha}|^4} \right) \left(\frac{|t_0^{a',\alpha'}|^2}{1 + |t_0^{a',\alpha'}|^4} \right) \\
\Lambda_{\text{Ins}}^F = & 1 - \frac{a_0^2}{R_{\alpha,\beta}^2} \left(\frac{|t_0^{a,\alpha}|^4}{1 + |t_0^{a,\alpha}|^4} \right) - \frac{a_0^2}{R_{\alpha',\beta}^2} \left(\frac{|t_0^{a',\alpha'}|^4}{1 + |t_0^{a',\alpha'}|^4} \right) \\
& - 2 \frac{a_0^3}{R_{\alpha,\beta} R_{\alpha',\beta} R_{\alpha,\alpha'}} \left(1 - |t_0^{a,\alpha}|^2 |t_0^{a',\alpha'}|^2 \right) \left(\frac{|t_0^{a,\alpha}|^2}{1 + |t_0^{a,\alpha}|^4} \right) \left(\frac{|t_0^{a',\alpha'}|^2}{1 + |t_0^{a',\alpha'}|^4} \right). \tag{48}
\end{aligned}$$

We deduce from (47) and (48) the value of the gap difference function defined by (43):

$$\delta_\beta = -\frac{1}{U} \frac{2\pi^2 \hbar^2}{ma_0^2} \left(1 - |t_0^{a,\alpha}|^2 |t_0^{a',\alpha'}|^2 \right) \frac{|t_0^{a,\alpha}|^2}{1 + |t_0^{a,\alpha}|^4} \frac{|t_0^{a',\alpha'}|^2}{1 + |t_0^{a',\alpha'}|^4} \frac{a_0^3}{R_{\alpha,\beta} R_{\alpha',\beta} R_{\alpha,\alpha'}}.$$

The physical values of the tunnel matrix elements are such that $|t_0^{a,\alpha}| |t_0^{a',\alpha'}| < 1$. As a consequence we obtain $\delta_\beta < 0$. Namely, we recover the perturbative result obtained by de Gennes for insulating ferromagnets. This constitutes an additional indication of the validity of our approach.

G. Role of phase averaging

The microscopic Green's function $\hat{g}^{\alpha,\beta}$ depends on the phase variables $\varphi_{\alpha,\beta}(\omega)$ and $\psi_{\alpha,\beta}(\omega)$ (see Eq. (16)). In the preceding subsections, we have assumed that these phases were fixed variables: $\varphi_{\alpha,\beta}(\omega) = -\pi/2$ and $\psi_{\alpha,\beta}(\omega) = 0$. The phases given by (15) and (17) are “fast variables” that oscillate rapidly on microscopic scales, as opposed to the slowly varying prefactor involving $1/R_{\alpha,\beta}$ in $\hat{g}_{\alpha,\beta}$ – see Eq. (16). Moreover in a multichannel model these phases are automatically averaged out when the summation over all channels is carried out. It is therefore a realistic realistic assumption to consider that the phase variables are *random quantities* [12], and to average the Gorkov functions over “phase disorder”.

1. Single channel problem

Let us start with the single channel problem represented on Fig. 2. The expression of the local Gorkov function was already given in Eq. (23). We need to evaluate $\langle\langle g^{\beta,\alpha,A} f^{\alpha,\beta,A} \rangle\rangle$ and $\langle\langle g^{\beta,\alpha,R} f^{\alpha,\beta,R} \rangle\rangle$, where $\langle\langle \rangle\rangle$ denotes the

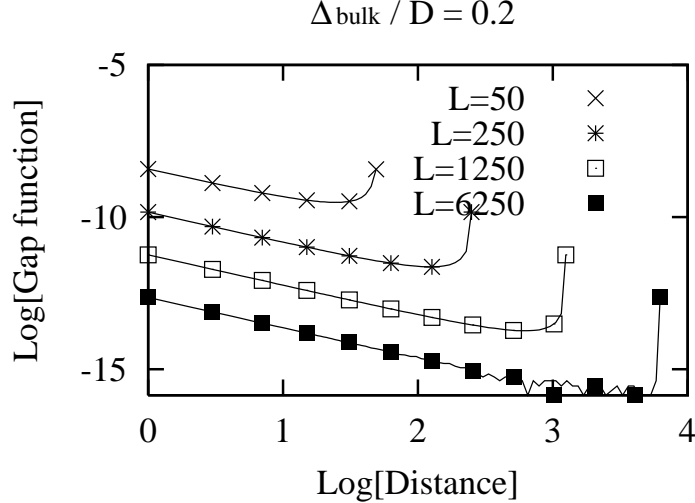


FIG. 11. Log-log plot of the variation of the gap difference function, with the geometry on Fig. 9 and with the same parameters as in the exact diagonalizations (see section IV): $\Delta_{\text{bulk}} = 0.2$ and $D = 1$ (see Fig. 14), and $t_0 = 0.05$. We used a pseudo-local gap kernel: $\Delta_0[\Delta] = \sqrt{\Delta_\alpha \Delta_\beta}$. The ferromagnetic gap is larger than the antiferromagnetic gap. With these parameters the ratio between the superconducting gap and the bandwidth is $\Delta_{\text{bulk}}/D = 0.2$.

averaging over phase disorder.

Let us first assume that the phases are symmetric: $\varphi_{\alpha,\beta}(\omega) = \varphi_{\beta,\alpha}(\omega)$, and $\psi_{\alpha,\beta}(\omega) = \psi_{\beta,\alpha}(\omega)$. This hypothesis leads to

$$g^{\beta,\alpha,A} f^{\alpha,\beta,A} = -\frac{1}{2} \left(\frac{ma_0^2}{2\pi^2 \hbar^2} \right) \left(\frac{a_0}{R_{\alpha,\beta}} \right)^2 \frac{\Delta_0}{\sqrt{\omega^2 - \Delta_0^2}} \left[e^{2i[\varphi_{\alpha,\beta}(\omega) + \psi_{\alpha,\beta}(\omega)]} - e^{2i\psi_{\alpha,\beta}(\omega)} \right], \quad (49)$$

from what we deduce $\langle\langle g^{\beta,\alpha,A} f^{\alpha,\beta,A} \rangle\rangle = 0$. Similarly, we find $\langle\langle g^{\beta,\alpha,R} f^{\alpha,\beta,R} \rangle\rangle = 0$, and we deduce that the superconducting gap does not depend on the transparency of the contact with the ferromagnet, with both the metallic and insulating ferromagnet model. Since this conclusion is not acceptable physically, we are lead to change the hypothesis and suppose that the phases are antisymmetric: $\varphi_{\alpha,\beta} = -\pi/2 + k_F R_{\alpha,\beta}$, $\varphi_{\beta,\alpha} = -\pi/2 - k_F R_{\alpha,\beta}$, and $\psi_{\alpha,\beta} = -\psi_{\beta,\alpha}$. Then, we obtain a finite expectation value for $\langle\langle g^{\beta,\alpha,A} f^{\alpha,\beta,A} \rangle\rangle$:

$$\langle\langle g^{\beta,\alpha,A} f^{\alpha,\beta,A} \rangle\rangle = \frac{1}{2} \left(\frac{ma_0^2}{2\pi^2 \hbar^2} \right) \left(\frac{a_0}{R_{\alpha,\beta}} \right)^2 \frac{\Delta_0}{\sqrt{\omega^2 - \Delta_0^2}}, \quad (50)$$

from what we deduce the self consistent superconducting order parameter in the local gap kernel approach:

$$\Delta_\beta = 2D \exp \left\{ -\frac{1}{U} \frac{2\pi^2 \hbar^2}{ma_0^2} \left[1 - \frac{1}{2} \left(\frac{a_0}{R_{\alpha,\beta}} \right)^2 \frac{t_0^2}{1+t_0^2} \right]^{-1} \right\}. \quad (51)$$

We see that the form of the gap profile is similar to Eq. (25), except for the coefficient 1/2 due to the average over phase disorder. Now we use antisymmetric phase variables to average out the phase disorder in the different types of two-channel heterostructures.

H. Two-channel problem with metallic ferromagnets

Using antisymmetric phase variables in the case of the two-channel heterostructure with metallic ferromagnets, we obtain

$$\Lambda_{\text{Metal}}^{\text{AF}} = 1 - \frac{a_0^2}{R_{\alpha,\beta}^2} \left(\frac{|t_0^{a,\alpha}|^2}{1+|t_0^{a,\alpha}|^2} \right) \sin^2(\varphi_{\alpha,\beta}) - \frac{a_0^2}{R_{\alpha',\beta}^2} \left(\frac{|t_0^{a',\alpha'}|^2}{1+|t_0^{a',\alpha'}|^2} \right) \sin^2(\varphi_{\alpha',\beta}) \quad (52)$$

$$\begin{aligned}
& + \frac{a_0^3}{R_{\alpha,\beta}R_{\alpha',\beta}R_{\alpha,\alpha'}} \left(\frac{|t_0^{a,\alpha}|^2}{1+|t_0^{a,\alpha}|^2} \right) \left(\frac{|t_0^{a',\alpha'}|^2}{1+|t_0^{a',\alpha'}|^2} \right) \sin(\varphi_{\alpha,\alpha'}) \cos(\varphi_{\beta,\alpha} + \varphi_{\alpha',\beta}) \\
\Lambda_{\text{Metal}}^{\text{F}} & = 1 - \frac{a_0^2}{R_{\alpha,\beta}^2} \left(\frac{|t_0^{a,\alpha}|^2}{1+|t_0^{a,\alpha}|^2} \right) \sin^2(\varphi_{\alpha,\beta}) - \frac{a_0^2}{R_{\alpha',\beta}^2} \left(\frac{|t_0^{a',\alpha'}|^2}{1+|t_0^{a',\alpha'}|^2} \right) \sin^2(\varphi_{\alpha',\beta}) \\
& + \frac{a_0^3}{R_{\alpha,\beta}R_{\alpha',\beta}R_{\alpha,\alpha'}} \left(\frac{|t_0^{a,\alpha}|^2}{1+|t_0^{a,\alpha}|^2} \right) \left(\frac{|t_0^{a',\alpha'}|^2}{1+|t_0^{a',\alpha'}|^2} \right) \{ \cos(\varphi_{\beta,\alpha} + \varphi_{\alpha,\alpha'}) \sin(\varphi_{\alpha',\beta}) + \cos(\varphi_{\beta,\alpha'} + \varphi_{\alpha',\alpha}) \sin(\varphi_{\alpha,\beta}) \}.
\end{aligned} \tag{53}$$

After averaging over phase disorder, we obtain

$$\begin{aligned}
\langle\langle \Lambda_{\text{Metal}}^{\text{AF}} \rangle\rangle & = 1 - \frac{1}{2} \frac{a_0^2}{R_{\alpha,\beta}^2} \left(\frac{|t_0^{a,\alpha}|^2}{1+|t_0^{a,\alpha}|^2} \right) - \frac{1}{2} \frac{a_0^2}{R_{\alpha',\beta}^2} \left(\frac{|t_0^{a',\alpha'}|^2}{1+|t_0^{a',\alpha'}|^2} \right) \\
& + \frac{1}{2} \frac{a_0^3}{R_{\alpha,\beta}R_{\alpha',\beta}R_{\alpha,\alpha'}} \left(\frac{|t_0^{a,\alpha}|^2}{1+|t_0^{a,\alpha}|^2} \right) \left(\frac{|t_0^{a',\alpha'}|^2}{1+|t_0^{a',\alpha'}|^2} \right)
\end{aligned} \tag{54}$$

$$\begin{aligned}
\langle\langle \Lambda_{\text{Metal}}^{\text{F}} \rangle\rangle & = 1 - \frac{1}{2} \frac{a_0^2}{R_{\alpha,\beta}^2} \left(\frac{|t_0^{a,\alpha}|^2}{1+|t_0^{a,\alpha}|^2} \right) - \frac{1}{2} \frac{a_0^2}{R_{\alpha',\beta}^2} \left(\frac{|t_0^{a',\alpha'}|^2}{1+|t_0^{a',\alpha'}|^2} \right) \\
& + \frac{a_0^3}{R_{\alpha,\beta}R_{\alpha',\beta}R_{\alpha,\alpha'}} \left(\frac{|t_0^{a,\alpha}|^2}{1+|t_0^{a,\alpha}|^2} \right) \left(\frac{|t_0^{a',\alpha'}|^2}{1+|t_0^{a',\alpha'}|^2} \right).
\end{aligned} \tag{55}$$

The form of the Gorkov functions is therefore similar to Eqs. (38) and (42), except for the 1/2 prefactors.

I. Two-channel problem with insulating ferromagnets

In the case of the two-channel heterostructure with insulating ferromagnets, we obtain

$$\begin{aligned}
\langle\langle \Lambda_{\text{Ins}}^{\text{AF}} \rangle\rangle & = 1 - \frac{1}{2} \frac{a_0^2}{R_{\alpha,\beta}^2} \left(\frac{|t_0^{a,\alpha}|^4}{1+|t_0^{a,\alpha}|^4} \right) - \frac{1}{2} \frac{a_0^2}{R_{\alpha',\beta}^2} \left(\frac{|t_0^{a',\alpha'}|^4}{1+|t_0^{a',\alpha'}|^4} \right) \\
& - \frac{1}{2} \frac{a_0^3}{R_{\alpha,\beta}R_{\alpha',\beta}R_{\alpha,\alpha'}} \left(1 - |t_0^{a,\alpha}|^2 |t_0^{a',\alpha'}|^2 \right) \left(\frac{|t_0^{a,\alpha}|^2}{1+|t_0^{a,\alpha}|^4} \right) \left(\frac{|t_0^{a',\alpha'}|^2}{1+|t_0^{a',\alpha'}|^4} \right)
\end{aligned} \tag{56}$$

$$\begin{aligned}
\langle\langle \Lambda_{\text{Ins}}^{\text{F}} \rangle\rangle & = 1 - \frac{1}{2} \frac{a_0^2}{R_{\alpha,\beta}^2} \left(\frac{|t_0^{a,\alpha}|^4}{1+|t_0^{a,\alpha}|^4} \right) - \frac{1}{2} \frac{a_0^2}{R_{\alpha',\beta}^2} \left(\frac{|t_0^{a',\alpha'}|^4}{1+|t_0^{a',\alpha'}|^4} \right) \\
& - \frac{a_0^3}{R_{\alpha,\beta}R_{\alpha',\beta}R_{\alpha,\alpha'}} \left(1 - |t_0^{a,\alpha}|^2 |t_0^{a',\alpha'}|^2 \right) \left(\frac{|t_0^{a,\alpha}|^2}{1+|t_0^{a,\alpha}|^4} \right) \left(\frac{|t_0^{a',\alpha'}|^2}{1+|t_0^{a',\alpha'}|^4} \right),
\end{aligned} \tag{57}$$

which differs from (47) and (48) only by the 1/2 coefficients.

J. “Mixed” junction with an insulating and a metallic ferromagnet

Let us now consider the “mixed” heterostructure on Fig. 5 in which the “a” electrode is metallic and the “b” electrode is insulating. It is straightforward to generalize the previous formalism to obtain

$$\begin{aligned}
\Lambda_{\text{Mixed}}^{\text{AF}} & = 1 - \frac{a_0^2}{R_{\alpha,\beta}^2} \left(\frac{|t_0^{a,\alpha}|^2}{1+|t_0^{a,\alpha}|^2} \right) \sin^2(\varphi_{\alpha,\beta}) \\
& + \frac{a_0^2}{R_{\alpha',\beta}^2} \left(\frac{|t_0^{a',\alpha'}|^2}{1+|t_0^{a',\alpha'}|^4} \right) \sin(\varphi_{\beta,\alpha'}) \left[\cos(\varphi_{\alpha',\beta}) - |t_0^{a',\alpha'}|^2 \sin(\varphi_{\alpha',\beta}) \right] \\
& + \frac{a_0^3}{R_{\alpha,\beta}R_{\alpha',\beta}R_{\alpha,\alpha'}} \left(\frac{|t_0^{a,\alpha}|^2}{1+|t_0^{a,\alpha}|^2} \right) \left(\frac{|t_0^{a',\alpha'}|^2}{1+|t_0^{a',\alpha'}|^4} \right) \sin(\varphi_{\alpha,\alpha'}) \left[\sin(\varphi_{\beta,\alpha} + \varphi_{\alpha',\beta}) + |t_0^{a',\alpha'}|^2 \cos(\varphi_{\beta,\alpha} + \varphi_{\alpha',\beta}) \right]
\end{aligned} \tag{58}$$

$$\begin{aligned}
\Lambda_{\text{Mixed}}^F &= 1 - \frac{a_0^2}{R_{\alpha,\beta}^2} \left(\frac{|t_0^{a,\alpha}|^2}{1 + |t_0^{a,\alpha}|^2} \right) \sin^2(\varphi_{\alpha,\beta}) \\
&+ \frac{a_0^2}{R_{\alpha',\beta}^2} \left(\frac{|t_0^{a',\alpha'}|^2}{1 + |t_0^{a',\alpha'}|^4} \right) \left[\cos(\varphi_{\beta,\alpha'}) \sin(\varphi_{\alpha',\beta}) - |t_0^{a',\alpha'}|^2 \sin(\varphi_{\alpha',\beta}) \sin(\varphi_{\beta,\alpha'}) \right] \\
&+ \frac{a_0^3}{R_{\alpha,\beta} R_{\alpha',\beta} R_{\alpha,\alpha'}} \left(\frac{|t_0^{a,\alpha}|^2}{1 + |t_0^{a,\alpha}|^2} \right) \left(\frac{|t_0^{a',\alpha'}|^2}{1 + |t_0^{a',\alpha'}|^4} \right) \times \\
&[\sin(\varphi_{\beta,\alpha} + \varphi_{\alpha,\alpha'}) \sin(\varphi_{\alpha',\beta}) + \sin(\varphi_{\beta,\alpha'} + \varphi_{\alpha',\alpha}) \sin(\varphi_{\alpha,\beta}) \\
&+ |t_0^{a',\alpha'}|^2 (\cos(\varphi_{\beta,\alpha} + \varphi_{\alpha,\alpha'}) \sin(\varphi_{\alpha',\beta}) + \cos(\varphi_{\beta,\alpha'} + \varphi_{\alpha',\alpha}) \sin(\varphi_{\alpha,\beta}))].
\end{aligned} \tag{59}$$

Averaging over phase disorder leads to

$$\begin{aligned}
\langle\langle \Lambda_{\text{Mixed}}^{\text{AF}} \rangle\rangle &= 1 - \frac{1}{2} \frac{a_0^2}{R_{\alpha,\beta}^2} \left(\frac{|t_0^{a,\alpha}|^2}{1 + |t_0^{a,\alpha}|^2} \right) - \frac{1}{2} \frac{a_0^2}{R_{\alpha',\beta}^2} \left(\frac{|t_0^{a',\alpha'}|^4}{1 + |t_0^{a',\alpha'}|^4} \right) \\
&+ \frac{1}{2} \frac{a_0^3}{R_{\alpha,\beta} R_{\alpha',\beta} R_{\alpha,\alpha'}} \left(\frac{|t_0^{a,\alpha}|^2}{1 + |t_0^{a,\alpha}|^2} \right) \left(\frac{|t_0^{a',\alpha'}|^4}{1 + |t_0^{a',\alpha'}|^4} \right)
\end{aligned} \tag{60}$$

$$\begin{aligned}
\langle\langle \Lambda_{\text{Mixed}}^F \rangle\rangle &= 1 - \frac{1}{2} \frac{a_0^2}{R_{\alpha,\beta}^2} \left(\frac{|t_0^{a,\alpha}|^2}{1 + |t_0^{a,\alpha}|^2} \right) \sin^2(\varphi_{\alpha,\beta}) + \frac{1}{2} \frac{a_0^2}{R_{\alpha',\beta}^2} \left(\frac{|t_0^{a',\alpha'}|^4}{1 + |t_0^{a',\alpha'}|^4} \right) \\
&+ \frac{a_0^3}{R_{\alpha,\beta} R_{\alpha',\beta} R_{\alpha,\alpha'}} \left(\frac{|t_0^{a,\alpha}|^2}{1 + |t_0^{a,\alpha}|^2} \right) \left(\frac{|t_0^{a',\alpha'}|^4}{1 + |t_0^{a',\alpha'}|^4} \right).
\end{aligned} \tag{61}$$

As a consequence $\delta_\beta > 0$: this heterostructure behaves like the full metallic heterostructure.

K. Interpretation in terms of Feynman diagrams

It is a relevant question to ask whether there are simple rules underlying the sign of the gap function in the different models. We show that the answer to this question is “yes” because the sign of the different terms in Λ^{AF} and Λ^F can be predicted from lowest order perturbation theory.

Let us start with the metallic model. We see from Eq. (28) and Eqs. (32) – (33) that the lowest order non local process renormalizing the anomalous propagator is given by

$$g^{\beta,\alpha} t^{\alpha,a} g_{1,1}^{a,a} t^{a,\alpha} f^{\alpha,\alpha'} t^{\alpha',a'} g_{2,2}^{a',a'} t^{a',\alpha'} g^{\alpha',\beta} \tag{62}$$

if the ferromagnets have an antiparallel spin orientation, and by

$$g^{\beta,\alpha} t^{\alpha,a} g_{1,1}^{a,a} t^{a,\alpha} g^{\alpha,\alpha'} t^{\alpha',a'} g_{1,1}^{a',a'} t^{a',\alpha'} f^{\alpha',\beta} \tag{63}$$

$$f^{\beta,\alpha} t^{\alpha,a} g_{1,1}^{a,a} t^{a,\alpha} g^{\alpha,\alpha'} t^{\alpha',a'} g_{1,1}^{a',a'} t^{a',\alpha'} g^{\alpha',\beta} \tag{64}$$

if the ferromagnets have a parallel spin orientation. The corresponding diagrams are shown on Fig. 12. Each of these diagrams contains four “ g ” propagators and one “ f ” propagator. As a consequence the sign of the coefficient of the non local term in Λ_{Metal}^F and $\Lambda_{\text{Metal}}^{\text{AF}}$ is positive (in agreement with Eqs. 38 and 42). Moreover there is one diagram involved in the case of parallel spin orientations, and two diagrams in the case of antiparallel spin orientations. This explains the origin of the factor of two appearing in the case of a parallel spin orientation – see Eqs. (38 and 42).

Let us now consider insulating ferromagnets. The lowest order diagrams are still given by (62), (63) and (64) but now $g^{a,a}$ and $g^{a',a'}$ are real numbers. As a consequence the sign of the non local term with insulating ferromagnets is opposite to the sign of the non local term with metallic ferromagnets, which is in agreement with Eqs. (47) and (48).

Finally in the mixed case the diagrams given by (62), (63) and (64) cancel because they are pure imaginary. Therefore we should look for the diagrams appearing in the next order. One of these diagrams is represented on Fig. 13. There are four “ g ” propagators involved. As a consequence the sign of this diagram is positive, which explains why the mixed junction behaves like the metallic junction. It should be also noted that the diagram on Fig. 13 is proportional to $|t^{a,\alpha}|^2 |t^{a',\alpha'}|^4$, which is in agreement with Eqs. (60) and (61).

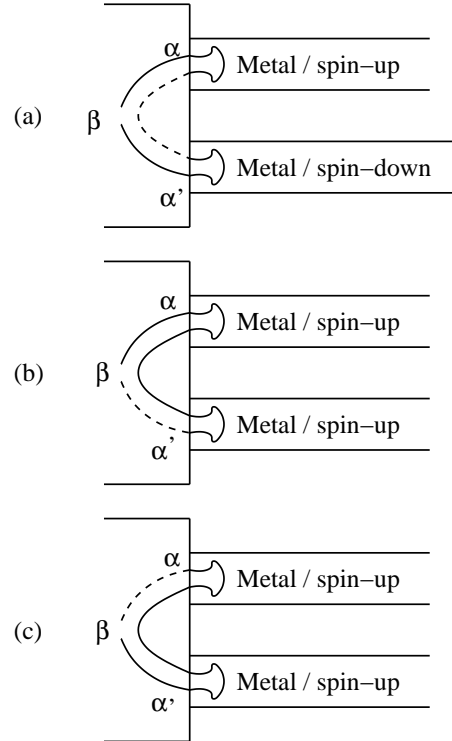


FIG. 12. The lowest order processes in the case of metallic ferromagnets. (a) corresponds to (62), (b) corresponds to (63), and (c) corresponds to (64).

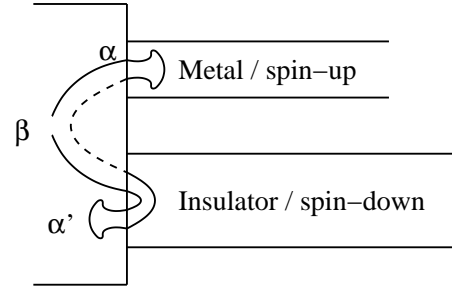


FIG. 13. The lowest order processes in the case of the mixed junction with antiparallel spin orientations.

IV. EXACT DIAGONALIZATIONS

Now we present a simulation based on exact diagonalizations in which we iterate the complete functional form of the self consistency equation (6) until a sufficient precision has been reached. The method is presented in sections IV A and IV B. The results are discussed in section IV C.

A. The generalized Bogoliubov-de Gennes equations

1. Bogoliubov-de Gennes Hamiltonian

Let us consider the BCS model (2) on a one dimensional lattice with L sites (see Fig. 9):

$$\hat{\mathcal{H}} - \mu \hat{N} = \sum_{\sigma, i=1}^L -t (c_{i+1,\sigma}^+ c_{i,\sigma} + c_{i,\sigma}^+ c_{i+1,\sigma}) + \sum_{i=1}^L \Delta_i (c_{i,\uparrow}^+ c_{i,\downarrow}^+ + c_{i,\downarrow} c_{i,\uparrow}) - \mu \hat{N}. \quad (65)$$

We consider a one dimensional geometry because we cannot treat numerically the two dimensional model because of computational limitations. Nevertheless, the principle of the method is valid also for two-dimensional models. It is convenient to use the notation

$$\check{\psi}_{\uparrow}^{+} = \left[c_{1,\uparrow}^{+}, \dots, c_{L,\uparrow}^{+}, c_{1,\downarrow}, \dots, c_{L,\downarrow} \right], \quad (66)$$

in which $\check{\psi}_{\uparrow}^{+}$ has $2L$ components. We can use (66) to obtain the generalized Bogoliubov-de Gennes Hamiltonian

$$\check{H} = \check{\psi}_{\uparrow}^{+} \check{K} \check{\psi}_{\uparrow} + \check{\psi}_{\uparrow}^{+} \check{\Delta} \check{\psi}_{\uparrow}, \quad (67)$$

where the kinetic term is

$$\check{K}_{i,j}^{1,1} = -t(\delta_{i,j+1} + \delta_{i,j-1}) + \mu\delta_{i,j} \quad (68)$$

$$\check{K}_{k,l}^{2,2} = t(\delta_{k,l+1} + \delta_{k,l-1}) - \mu\delta_{k,l} \quad (69)$$

$$\check{K}_{i,k}^{1,2} = \check{K}_{k,i}^{2,1} = 0, \quad (70)$$

and the pairing term is

$$\check{\Delta}_{i,j}^{1,1} = \check{\Delta}_{i,j}^{2,2} = 0 \quad (71)$$

$$\check{\Delta}_{i,k}^{1,2} = \check{\Delta}_{k,i}^{2,1} = \Delta_i\delta_{i,k}. \quad (72)$$

Similarly to the Nambu representation, we have used the label “1” for the “electronic” components of $\check{\psi}$ and the label “2” for the “hole” components. We implicitly doubled the space coordinates: the labels i, j correspond to the electronic component and the labels k, l correspond to the hole component. The symbol $\delta_{i,k}$ means that i and k represent the same site on the lattice but belong to a different Nambu component.

2. Spectral representations

The eigenvectors of the Bogoliubov-de Gennes Hamiltonian (67) take the form

$$|\psi_{\alpha}\rangle = \sum_{i=1}^L R_{\alpha,i} |e_i\rangle + \sum_{k=1}^L R_{\alpha,k} |e_k\rangle \quad (73)$$

$$|\psi_{\beta}\rangle = \sum_{i=1}^L R_{\beta,i} |e_i\rangle + \sum_{k=1}^L R_{\beta,k} |e_k\rangle, \quad (74)$$

where the eigenvalues are such that $\lambda_{\alpha} > 0$ and $\lambda_{\beta} < 0$. In this notation there are L kets $|e_i\rangle$ associated to the first component of the Nambu representation, and there are L kets $|e_k\rangle$ associated to the second component of the Nambu representation. We deduce from Eqs. (73) and (74) the form of the quasiparticle operators

$$\Gamma_{\alpha,\downarrow}^{+} = \sum_i R_{\alpha,i} c_{i,\uparrow} + \sum_k R_{\alpha,k} c_{k,\downarrow}^{+} \quad (75)$$

$$\Gamma_{\beta,\uparrow} = \sum_i R_{\beta,i} c_{i,\uparrow} + \sum_k R_{\beta,k} c_{k,\downarrow}^{+} \quad (76)$$

which diagonalize the Bogoliubov-de Gennes Hamiltonian

$$\hat{\mathcal{H}} = \sum_{\alpha} \lambda_{\alpha} \Gamma_{\alpha,\downarrow}^{+} \Gamma_{\alpha,\downarrow} - \sum_{\beta} \lambda_{\beta} \Gamma_{\beta,\uparrow}^{+} \Gamma_{\beta,\uparrow}.$$

The spectral representation of the Green’s function (4) can be expressed in terms of the matrix R :

$$g_{i,j}^{A,1,1} = \sum_{\beta} \frac{R_{\beta,i} R_{\beta,j}}{\omega + i\eta - [\mu + |E_{\beta}|]} + \sum_{\alpha} \frac{R_{\alpha,i} R_{\alpha,j}}{\omega + i\eta - [\mu - E_{\alpha}]} \quad (77)$$

$$g_{i,k}^{A,1,2} = \sum_{\beta} \frac{R_{\beta,i} R_{\beta,k}}{\omega + i\eta - [\mu + |E_{\beta}|]} + \sum_{\alpha} \frac{R_{\alpha,i} R_{\alpha,k}}{\omega + i\eta - [\mu - E_{\alpha}]} \quad (78)$$

It is easy to show that (77) and (78) reduce to (10) and (11) in the presence of translational invariance.

B. Evaluation of the Green's functions

1. Evaluation of a spectral representation:

The Green's functions are obtained from (77) and (78) in terms of their poles ω_n and residues R_n :

$$g_0^A(\omega) = \sum_n \frac{R_n}{\omega - \omega_n - i\eta}. \quad (79)$$

To make the integration over energy, we go to the limit of zero dissipation ($\eta \rightarrow 0$) and use the identity $1/[\omega - \omega_n - i\eta] = \mathcal{P}/[\omega - \omega_n] + i\pi\delta(\omega - \omega_n)$. To show that the principal part cancels if $\omega > \Delta$, we come back to the particular case where the superconducting order parameter is uniform: $\Delta_\beta \equiv \Delta_0$ for all β (see section II D). We start from (11) and make the replacement

$$\frac{1}{\omega - (\mu_S + E_k) - i\eta} \rightarrow i\pi\delta(\omega - (\mu_S + E_k)) \quad (80)$$

$$\frac{1}{\omega - (\mu_S - E_k) - i\eta} \rightarrow i\pi\delta(\omega - (\mu_S - E_k)). \quad (81)$$

The Green's function (10) becomes

$$g_{\alpha,\beta}^A \rightarrow i\pi \frac{1}{\mathcal{N}} \sum_{\vec{k}} e^{i\vec{k} \cdot (\vec{x}_\alpha - \vec{x}_\beta)} [(u_k)^2 \delta(\omega - (\mu_S + E_k)) + (v_k)^2 \delta(\omega - (\mu_S - E_k))]. \quad (82)$$

After using the δ -function (82) and performing the integral over wave vector we recover the form (16) of the Green's function in which the term proportional to $\cos\varphi$ has been discarded. This does not constitute a source of problem because we know from section III that the envelope of the $2k_F$ -oscillations is the same in the presence or absence of the $\cos\varphi$ term. Therefore if $\omega > \Delta$, Eq. (79) can be replaced by

$$g_0^A(\omega) = i\pi \sum_n R_n \delta(\omega - \omega_n). \quad (83)$$

2. Evaluation of the δ -functions

To evaluate the δ -function in (83), we replace $\delta(\omega - \omega_n)$ by $\delta_\eta(\omega)$, where $\delta_\eta(\omega)$ is a function having a width η in energy, and normalized to unity: $\int \delta_\eta(\omega) d\omega = 1$. For instance $\delta_\eta(\omega)$ can be chosen as a Lorentzian or a Gaussian. One should however keep in mind that the Lorentzian or the Gaussian will be computed $2L$ times to evaluate a Green's function at a single energy ω . Such evaluations will be performed an enormous amount of time in the program. To optimize this part of the program, it is useful to use a function $\delta_\eta(\omega)$ that is finite only in the interval $[-\eta, \eta]$ and vanishes outside this energy interval. The simplest choice is given by

$$\delta_\eta(\omega) = \frac{3}{4\eta} \left[1 - \left(\frac{\omega}{\eta} \right)^2 \right] \text{ if } |\omega| < \eta. \quad (84)$$

C. Results

We consider the geometry represented in Fig. 9 in which a one dimensional superconductor on an open segment with L sites is connected to two ferromagnetic metals. The superconductor is described by the BCS tight-binding Hamiltonian (2). We note $t_0 = t_{a,\alpha}/t = t_{a',\alpha'}/t$ the tunnel matrix element connecting the ferromagnets and the superconductor, normalized to the bandwidth of the superconductor. Low transparency interfaces correspond to $t_0 \ll 1$ and high transparency interfaces correspond to $t_0 \sim 1$.

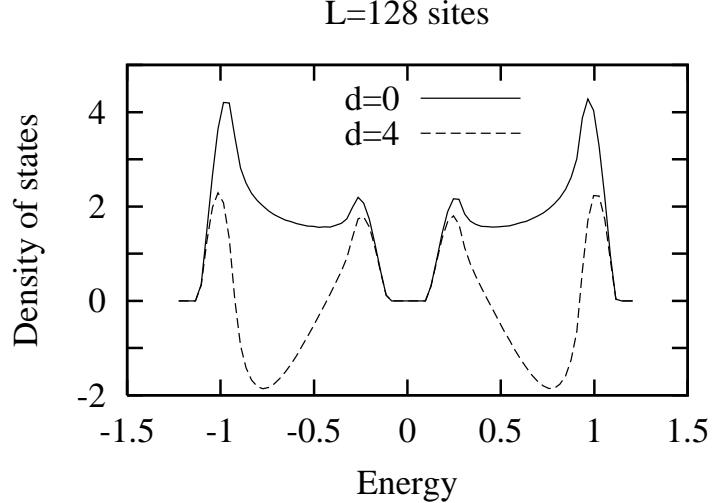


FIG. 14. Energy dependence of the density of state $\rho_g^{\alpha,\beta}$, for two values of the distance between the sites α and β . We used periodic boundary conditions, with $L = 128$ sites. The hopping energy is $t = 0.5$, the superconducting gap $\Delta_0 = 0.2$ is uniform and the level broadening is $\eta = 0.1$.

1. Density of states

We have shown on Fig. 14 the energy dependence of the density of states $\rho_g^{\alpha,\beta}$ associated to the ordinary propagator (see section II B) in the presence of a uniform gap profile $\Delta_\beta \equiv \Delta_0$ for all β , and with $L = 128$ sites. We can check on this figure that the different parameters of the simulation are compatible with each other. Namely, the level broadening η is sufficiently small to have a well-defined superconducting gap. The level broadening is also sufficiently large for quasiparticle states to form a continuous band. Because of these two constraints, it is in practice impossible to use realistic parameters as we did for the local approach in section III (see Fig. 3). Using realistic parameters would require too large system sizes.

Finally, the calculation of the superconducting order parameter in the gap kernel approaches presented in section III were based on the logarithmic divergence of the integrated Gorkov function at high energy (see section II D 4). By contrast low energy degrees of freedom play a relevant role in our simulation. One of the questions that will be answered by the exact diagonalizations is to determine whether low energy degrees of freedom (probed by the numerical simulation with strong finite size effects) have the same physics as high energy degrees of freedom (probed by the local or pseudo-local approaches).

2. Gap profile

The gap profile is shown on Fig. 15 for $L = 128$ sites. We obtained similar results for $L = 32$ and $L = 64$ sites. The gap profile obtained with exact diagonalizations is qualitatively similar to the gap kernel approaches presented in section III. Namely, the superconducting order parameter is reduced close to the interface with the ferromagnets and we obtain $2k_F$ oscillations in the gap profile.

3. Gap difference function

We have shown on Fig. 16 the variation of the gap difference function with $L = 128$ sites. Similar results have been obtained with $L = 32$ and $L = 64$ sites. For each site β in the superconductor, we have calculated the superconducting order parameters Δ_β^F and Δ_β^{AF} with parallel and antiparallel spin orientations in the two ferromagnetic electrodes. From what we deduce the value of the gap difference function δ_β defined by (43). The difficulty of the calculation is to iterate the process on Fig. 1 until a sufficient precision has been obtained. The relative error made on the determination of the order parameters should be several orders of magnitude smaller than the gap difference function.

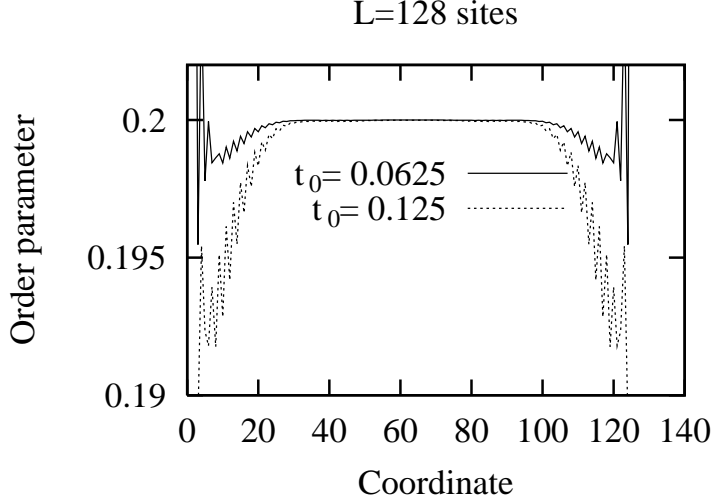


FIG. 15. Self consistent gap profile with $L = 128$ sites and two values of t_0 : $t_0 = 0.0625$ (solid line) and $t_0 = 0.125$ (dotted line). The other parameters are the same as on Fig. 14. The difference between the parallel and the antiparallel superconducting order parameters cannot be distinguished on the scale of the figure.

We made the simulations with two values of the normalized hopping between the superconductor and the ferromagnet (see Fig. 16). We also tried larger values of the interface transparencies but the algorithm did not converge. The clarification of this point is left as an open question for future work. From the result presented on Fig. 16 we deduce that

- (i) With all available sizes and interface transparencies, the gap difference function defined by (43) is positive, meaning that *the gap is larger in the ferromagnetic alignment*. This is opposite to the de Gennes model.
- (ii) The gap difference function tends to zero in the bulk of the superconductor. The cross-over between the surface and bulk behavior is controlled by a length scale which is of order 10 on Fig. 16. This length scale should be identified to the superconducting coherence length defined by Eq. (14).
- (iii) The numerical results are in a qualitative agreement with the gap kernel approaches presented in section III and support the existence of a low temperature regime dominated by pair correlations, not described by the de Gennes model.

V. CONCLUSION: RELATION WITH THE NON LOCAL PROXIMITY EFFECT

To summarize, we have provided a detailed investigation of F/S/F trilayers with metallic ferromagnets. The basic physics has been given in the introductory section and the remaining of the article was devoted to solve a microscopic model. We found that the physics of the metallic heterostructure was dominated by pair correlations, not by pair breaking. This behavior was obtained with several complementary approaches:

- (i) *The local kernel approximation* (see section III) in which we used realistic parameters ($\Delta_{\text{bulk}}/D = 10^{-4}$).
- (ii) *Exact diagonalizations* (see section IV) that were limited to small sizes and an artificially large value of Δ_{bulk}/D ($\Delta_{\text{bulk}}/D = 0.2$).
- (iii) *A non local gap kernel approximation* (see section III D) in which we could use realistic parameters to confirm the local kernel approximation result, and artificially large values of Δ_{bulk}/D to confirm the exact diagonalizations.

Our model would apply to a situation in which orbital depairing can be neglected. This situation is realized in type-II superconductor in a thin film geometry and with the magnetization of the ferromagnets parallel to the superconducting film [6]. In this situation, it is also legitimate to neglect spin orbit scattering as we did with metallic ferromagnets.

As proposed in Ref. [4], the strength of pair correlations can be characterized by the non local Gorkov functions $[G_{i,j}^{+,-}]_{1,2}$ and $[G_{i,j}^{+,-}]_{2,1}$. The sites i and j can be in any of the electrodes, either ferromagnetic or superconducting.

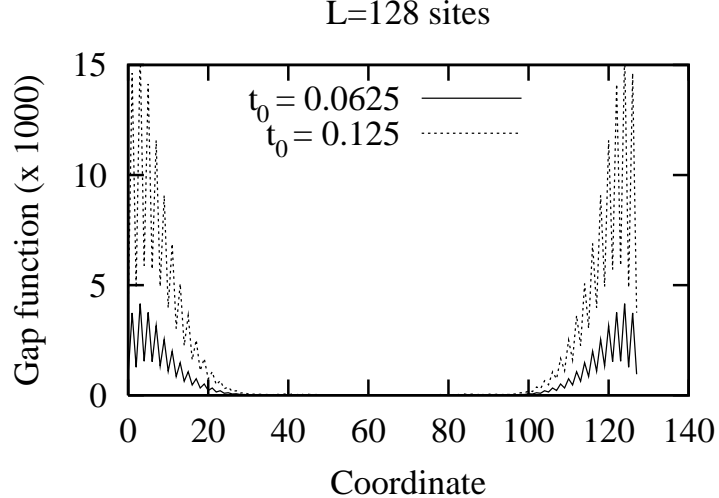


FIG. 16. Variation of the gap difference function with $L = 128$ sites in the superconductor. The parameters are identical to Fig. 15.

Since the ferromagnetic electrodes break spin rotational symmetry, we need to introduce *a priori* two correlation matrices:

$$K_{i,j}^{1,2}(\omega) = \frac{1}{n_F(\omega - \mu)} \frac{1}{2i\pi} [G_{i,j}^{+,-}(\omega)]_{1,2} \quad (85)$$

$$K_{i,j}^{2,1}(\omega) = \frac{1}{n_F(\omega - \mu)} \frac{1}{2i\pi} [G_{i,j}^{+,-}(\omega)]_{2,1}. \quad (86)$$

The two matrices $\hat{K}^{1,2}(\omega)$ and $\hat{K}^{2,1}(\omega)$ can be deduced from each other by the relation $\hat{K}_{i,j}^{1,2}(\omega) = \hat{K}_{j,i}^{2,1}(\omega)$. Therefore, we use only $\hat{K}^{1,2}(\omega)$ in the following and use the notation $\hat{K}(\omega)$ instead of $\hat{K}^{1,2}(\omega)$.

The matrix of Gorkov functions relevant to the three-terminal geometry takes the following form:

$$\hat{K}(\omega) = \begin{pmatrix} K_{\beta_1, \beta_2}(\omega) & K_{\beta, b'}(\omega) \\ K_{b, \beta}(\omega) & K_{b, b'}(\omega) \end{pmatrix}, \quad (87)$$

where β , β_1 , and β_2 are three arbitrary sites in the superconductor; a_1 , a_2 and b are three arbitrary sites in electrode “ a ”; a'_1 , a'_2 and b' are three arbitrary sites in electrode “ a' ” (see Fig. 17). We note $\hat{K}^{(<)}$ (ω) and $\hat{K}^{(>)}$ (ω) the matrices of Gorkov functions for $\omega < \Delta$ and $\omega > \Delta$ respectively.

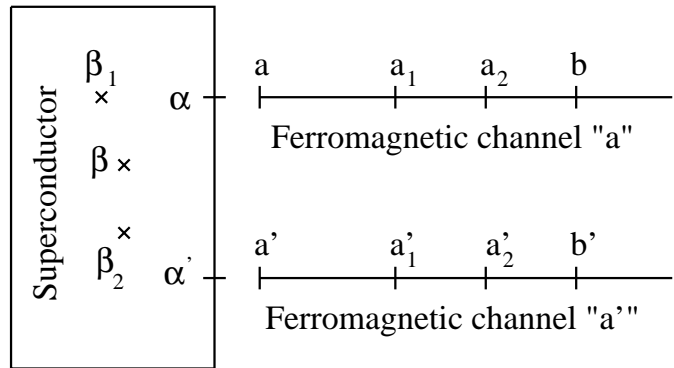


FIG. 17. The notation used in the parameterization of the matrix of Gorkov functions.

Let us first assume that the two ferromagnetic electrodes are metallic. In the case of an antiparallel spin orientation, the matrices of Gorkov functions are found to be

$$\hat{K}^{(<),\text{Metal,AF}}(\omega) = \begin{pmatrix} K_{\beta_1,\beta_2}^{(<),\text{Metal,AF}}(\omega) & K_{\beta,b'}^{(<),\text{Metal,AF}}(\omega) \\ K_{b,\beta}^{(<),\text{Metal,AF}}(\omega) & K_{b,b'}^{(<),\text{Metal,AF}}(\omega) \end{pmatrix}, \quad (88)$$

and

$$\hat{K}^{(>),\text{Metal,AF}}(\omega) = \begin{pmatrix} K_{\beta_1,\beta_2}^{(>),\text{Metal,AF}}(\omega) & 0 \\ 0 & K_{b,b'}^{(>),\text{Metal,AF}}(\omega) \end{pmatrix}. \quad (89)$$

The extra diagonal elements of $\hat{K}^{(>),\text{Metal,AF}}(\omega)$ are vanishing to all orders. The other matrix elements can be evaluated to lowest order in the tunnel amplitude:

$$K_{\beta_1,\beta_2}^{(<),\text{Metal,AF}}(\omega) = g^{\beta_1,\alpha} t^{\alpha,a} \rho_{1,1}^{a,a} t^{a,\alpha} f^{\alpha,\beta_2} + f^{\beta_1,\alpha'} t^{\alpha',a'} \rho_{2,2}^{a',a'} t^{a',\alpha'} g^{\alpha',\beta_2} \quad (90)$$

$$K_{\beta,b'}^{(<),\text{Metal,AF}}(\omega) = -f^{\beta,\alpha'} t^{\alpha',a'} \rho_{2,2}^{a',b'} \quad (91)$$

$$K_{b,\beta}^{(<),\text{Metal,AF}}(\omega) = \rho_{1,1}^{b,a} t^{a,\alpha} f^{\alpha,\beta} \quad (92)$$

$$K_{b,b'}^{(<),\text{Metal,AF}}(\omega) = \pi^2 \rho_{1,1}^{b,a} t^{a,\alpha} g^{\alpha,\alpha} t^{\alpha,a} \rho_{1,1}^{a,a} t^{a,\alpha} f^{\alpha,\alpha'} t^{\alpha',a'} \rho_{2,2}^{a',b'} + \pi^2 \rho_{1,1}^{b,a} t^{a,\alpha} f^{\alpha,\alpha'} t^{\alpha',a'} \rho_{2,2}^{a',a'} t^{a',\alpha'} g^{\alpha',\alpha'} t^{\alpha',a'} \rho_{2,2}^{a',b'} \quad (93)$$

$$K_{\beta_1,\beta_2}^{(>),\text{Metal,AF}}(\omega) = \rho_f^{\beta_1,\beta_2} \quad (94)$$

$$K_{b,b'}^{(>),\text{Metal,AF}}(\omega) = \pi^2 \rho_{1,1}^{b,a} t^{a,\alpha} \rho_f^{\alpha,\alpha'} t^{\alpha',a'} \rho_{2,2}^{a',b'}. \quad (95)$$

In the case of metallic ferromagnets having a parallel spin orientation, we obtain

$$\hat{K}^{(<),\text{Metal,F}}(\omega) = \begin{pmatrix} K_{\beta_1,\beta_2}^{(<),\text{Metal,F}}(\omega) & 0 \\ K_{b,\beta}^{(<),\text{Metal,F}}(\omega) & 0 \end{pmatrix}, \quad (96)$$

and

$$\hat{K}^{(>),\text{Metal,F}}(\omega) = \begin{pmatrix} K_{\beta_1,\beta_2}^{(>),\text{Metal,F}}(\omega) & 0 \\ 0 & 0 \end{pmatrix}, \quad (97)$$

where the non vanishing Gorkov functions are given by

$$K_{\beta_1,\beta_2}^{(<),\text{Metal,F}}(\omega) = g^{\beta_1,\alpha} t^{\alpha,a} \rho_{1,1}^{a,a} t^{a,\alpha} f^{\alpha,\beta_2} + g^{\beta_1,\alpha'} t^{\alpha',a'} \rho_{1,1}^{a',a'} t^{a',\alpha'} f^{\alpha',\beta_2} \quad (98)$$

$$K_{b,\beta}^{(<),\text{Metal,F}}(\omega) = \rho_{1,1}^{b,a} t^{a,\alpha} f^{\alpha,\beta} \quad (99)$$

$$K_{\beta_1,\beta_2}^{(>),\text{Metal,F}}(\omega) = \rho_f^{\beta_1,\beta_2}. \quad (100)$$

Let us consider now two insulating ferromagnetic electrodes, and start with an antiparallel spin orientation. We obtain

$$\hat{K}^{(<),\text{Ins,AF}}(\omega) = \begin{pmatrix} 0 & 0 \\ 0 & 0 \end{pmatrix}, \quad (101)$$

and

$$\hat{K}^{(>),\text{Ins,AF}}(\omega) = \begin{pmatrix} K_{\beta_1,\beta_2}^{(>),\text{Ins,AF}}(\omega) & K_{\beta,b'}^{(>),\text{Ins,AF}}(\omega) \\ K_{b,\beta}^{(>),\text{Ins,AF}}(\omega) & K_{b,b'}^{(>),\text{Ins,AF}}(\omega) \end{pmatrix}, \quad (102)$$

where the non vanishing Gorkov functions are given by

$$K_{\beta_1,\beta_2}^{(>),\text{Ins,AF}}(\omega) = \rho_f^{\beta_1,\beta_2} \quad (103)$$

$$K_{\beta,b'}^{(>),\text{Ins,AF}}(\omega) = -f^{\beta,\alpha'} t^{\alpha',a'} g_{2,2}^{a',b'} \quad (104)$$

$$K_{b,\beta}^{(>),\text{Ins,AF}}(\omega) = g_{1,1}^{b,a} t^{a,\alpha} f^{\alpha,\beta} \quad (105)$$

$$K_{b,b'}^{(>),\text{Ins,AF}}(\omega) = -g_{1,1}^{b,a} t^{a,\alpha} \rho_f^{\alpha,\alpha'} t^{\alpha',a'} g_{2,2}^{a',b'}. \quad (106)$$

Finally, in the case of insulating ferromagnets in the parallel configuration, we obtain

$$\hat{K}^{(<),\text{Ins},\text{F}}(\omega) = \begin{pmatrix} 0 & 0 \\ 0 & 0 \end{pmatrix}, \quad (107)$$

and

$$\hat{K}^{(>),\text{Ins},\text{F}}(\omega) = \begin{pmatrix} K_{\beta_1,\beta_2}^{(>),\text{Ins},\text{F}}(\omega) & 0 \\ K_{b,\beta}^{(>),\text{Ins},\text{F}}(\omega) & 0 \end{pmatrix}, \quad (108)$$

with

$$K_{\beta_1,\beta_2}^{(>),\text{Ins},\text{F}}(\omega) = \rho_f^{\beta_1,\beta_2} \quad (109)$$

$$K_{b,\beta}^{(>),\text{Ins},\text{F}}(\omega) = g_{1,1}^{b,a} t^{a,\alpha} \rho_f^{\alpha,\beta}. \quad (110)$$

We make the following comments:

- (i) As expected, there is no proximity effect associated to insulating ferromagnets, which can be seen from the fact that the matrices of Gorkov functions $\hat{K}^{(<)}$ given by (107) and (101) are vanishing to all orders below the superconducting gap. This is due to the fact that it is not possible to generate a proximity effect in the presence of evanescent states.
- (ii) By contrast in the case of the metallic heterostructure the matrices of Gorkov functions (96) and (96) are non vanishing below the superconducting gap. This means that in this case there is a proximity effect induced in the ferromagnetic electrodes.
- (iii) Comparing (88) and (96) we see that with metallic ferromagnets the Gorkov function $K_{b,b'}^{(>),\text{Metal},\text{AF}}$ is vanishing in the case of a parallel spin orientation while it takes a finite value with an antiparallel spin orientation. This is due to the fact that the parallel spin orientation is not compatible with the formation of Cooper pair correlations.
- (iv) From Eqs. (95) and (106) we see that $K_{b,b'}^{(>),\text{Metal},\text{AF}} < 0$ while $K_{b,b'}^{(>),\text{Ins},\text{AF}} > 0$. This means that the metallic heterostructure favors antiferromagnetic correlations among the ferromagnets while the insulating heterostructure favors ferromagnetic correlations, which is in agreement with the sign of the gap difference function discussed in the article.
- (v) It can be seen from Eqs. (93) and (95) that $K_{b,b'}^{(<),\text{Metal},\text{AF}}(\omega)$ is equal to $K_{b,b'}^{(>),\text{Metal},\text{AF}}(\omega)$, plus a disconnected contribution. Therefore, the microscopic process involved in the non local proximity effect is *identical* to the microscopic process involved in the renormalization of the superconducting order parameter. The former involves energies smaller than the superconducting gap and the latter involves energies larger than the superconducting gap.

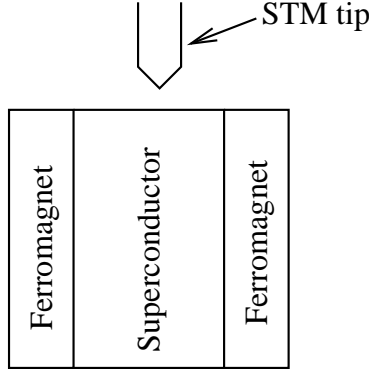


FIG. 18. Schematic representation of the STM experiment proposal.

To end-up we can propose two experiments that could be done in a near future:

- (i) A STM tip can be used to make a local spectroscopy of the superconductor similar to [21] and determine how the local density of states depends on the relative orientation of the ferromagnets (see Fig. 18). Another possibility is to use planar tunnel junctions similar to [22] to make a local spectroscopy of the superconductor.
- (ii) Perpendicular to plane dc transport across the F/S/F trilayer can also be used, both in the tunnel and Andreev reflection regimes.

These two possibilities require further theoretical developments that will be the subject of a future publication [20].

Finally, let us mention two recent theoretical articles [23] in which Usadel equations have been used to treat F/S/F heterostructures in the diffusive regime. These authors have apparently not incorporated the possibility of non local pair correlations induced in the ferromagnetic electrodes as we did in our approach, which might explain the differences regarding the sign of the gap ratio.

ACKNOWLEDGMENTS

The authors wish to thank D. Feinberg for fruitful discussions and for pointing out to them the relation with the insulating ferromagnet model solved in Ref. [1]. The authors also acknowledge a fruitful discussion with J.C. Cuevas who pointed out to them the possibility of using an equilibrium formalism rather than the Keldysh formalism.

APPENDIX A: EXPRESSION OF THE KELDYSH PROPAGATORS

The goal of this appendix is to rederive the main results of this article with the non equilibrium form (5) of the Gorkov function, rather than the equilibrium Gorkov function (7). This formalism based on non equilibrium Green's functions is more general than the equilibrium Green's function formalism because it can also be applied to non equilibrium problems. A detailed investigation of this issue will be presented in the future. Here, we want to show that both formalisms coincide for the equilibrium problem, which constitutes also a test of the calculations presented in the main body of the article.

1. One-channel problem

Let us first consider the single channel model (see Fig. 2). The renormalized propagator is the solution of the Dyson equation

$$\hat{G}^{a,a} = \hat{g}^{a,a} + \hat{g}^{a,a} \hat{t}^{a,\alpha} \hat{g}^{\alpha,\alpha} \hat{t}^{\alpha,a} \hat{G}^{a,a},$$

from what we deduce $G_{1,1}^{a,a} = g_{1,1}^{a,a}/\mathcal{D}$, with \mathcal{D} given by (24). The Dyson-Keldysh equation associated to an arbitrary site in the superconductor takes the form

$$\hat{G}_{\beta,\beta}^{+,-} = \hat{g}_{\beta,\beta}^{+,-} + \hat{g}_{\beta,\alpha}^{+,-} \hat{t}_{\alpha,a} \hat{G}_{a,\beta}^A + \hat{G}_{\beta,a}^R \hat{t}_{\alpha,a} \hat{g}_{\alpha,\beta}^{+,-} + \hat{G}_{\beta,a}^R \hat{t}_{a,\alpha} \hat{g}_{\alpha,\alpha}^{+,-} \hat{t}_{\alpha,a} \hat{G}_{a,\beta}^A + \hat{G}_{\beta,\alpha}^R \hat{t}_{\alpha,a} \hat{g}_{a,a}^{+,-} \hat{t}_{a,\alpha} \hat{G}_{\alpha,\beta}^A. \quad (\text{A1})$$

Evaluating the five terms in (A1) leads to

$$\begin{aligned} G_{\beta,\beta}^{+,-} = & 2i\pi n_F(\omega - \mu_S) \left\{ \rho_f^{\beta,\beta} + |t_{a,\alpha}|^2 \frac{1}{\mathcal{D}^A} g_{1,1}^{a,a,A} f^{\alpha,\beta,A} \rho_g^{\beta,\alpha} + |t_{a,\alpha}|^2 \frac{1}{\mathcal{D}^R} g_{1,1}^{a,a,R} g^{\beta,\alpha,R} \rho_f^{\alpha,\beta} \right. \\ & \left. + |t^{a,\alpha}|^4 \frac{1}{\mathcal{D}^A \mathcal{D}^R} g_{1,1}^{a,a,A} g_{1,1}^{a,a,R} g^{\beta,\alpha,R} f^{\alpha,\beta,A} \rho_g^{\alpha,\alpha} \right\} + 2i\pi n_F(\omega - \mu_a) |t^{a,\alpha}|^2 \frac{1}{\mathcal{D}^A \mathcal{D}^R} g^{\beta,\alpha,R} f^{\alpha,\beta,A} \rho_{1,1}^{a,a}. \end{aligned} \quad (\text{A2})$$

The final step is to show that with $\mu_a = \mu_S$ this expression coincides with (23).

2. Two-channel problem with antiparallel magnetizations

The Dyson-Keldysh equation associated to an arbitrary site β in the superconductor is the following:

$$\begin{aligned}\hat{G}_{\beta,\beta}^{+,-} &= \hat{g}_{\beta,\beta}^{+,-} + \hat{g}_{\beta,\alpha}^{+,-}\hat{t}_{\alpha,a}\hat{G}_{a,\beta}^A + \hat{g}_{\beta,\alpha'}^{+,-}\hat{t}_{\alpha',a'}\hat{G}_{a',\beta}^A + \hat{G}_{\beta,a}^R\hat{t}_{a,\alpha}\hat{g}_{\alpha,\beta}^{+,-} + \hat{G}_{\beta,a'}^R\hat{t}_{a',\alpha'}\hat{g}_{\alpha',\beta}^{+,-} + \hat{G}_{\beta,a}^R\hat{t}_{a,\alpha}\hat{g}_{\alpha,\alpha}^{+,-}\hat{t}_{\alpha,a}\hat{G}_{a,\beta}^A \\ &+ \hat{G}_{\beta,a'}^R\hat{t}_{a',\alpha'}\hat{g}_{\alpha',\alpha'}^{+,-}\hat{t}_{\alpha',a'}\hat{G}_{a',\beta}^A + \hat{G}_{\beta,a}^R\hat{t}_{a,\alpha}\hat{g}_{\alpha,\alpha'}^{+,-}\hat{t}_{\alpha',a'}\hat{G}_{a',\beta}^A + \hat{G}_{\beta,a'}^R\hat{t}_{a',\alpha'}\hat{g}_{\alpha',\alpha'}^{+,-}\hat{t}_{\alpha,a}\hat{G}_{a,\beta}^A \\ &+ \hat{G}_{\beta,\alpha}^R\hat{t}_{\alpha,a}\hat{g}_{a,a}^{+,-}\hat{t}_{a,\alpha}\hat{G}_{\alpha,\beta}^A + \hat{G}_{\beta,\alpha'}^R\hat{t}_{\alpha',a'}\hat{g}_{a',a'}^{+,-}\hat{t}_{a',\alpha'}\hat{G}_{\alpha',\beta}^A.\end{aligned}\quad (\text{A3})$$

We need the expression of the following renormalized Green's functions:

$$\hat{G}^{\beta,a} = t^{a,\alpha}g_{1,1}^{a,a} \begin{bmatrix} \tilde{g}^{\beta,\alpha} & 0 \\ \tilde{f}^{\beta,\alpha} & 0 \end{bmatrix} \quad (\text{A4})$$

$$\hat{G}^{\beta,a'} = -t^{a',\alpha'}g_{2,2}^{a',a'} \begin{bmatrix} 0 & \tilde{f}^{\beta,\alpha'} \\ 0 & \tilde{g}^{\beta,\alpha'} \end{bmatrix} \quad (\text{A5})$$

$$\hat{G}^{\alpha,\beta} = \begin{bmatrix} \tilde{g}^{\alpha,\beta} & \tilde{f}^{\alpha,\beta} \\ G_{2,1}^{\alpha,\beta} & G_{2,2}^{\alpha,\beta} \end{bmatrix} \quad (\text{A6})$$

$$\hat{G}^{\beta,\alpha} = \begin{bmatrix} \tilde{g}^{\beta,\alpha} & \tilde{G}_{1,2}^{\beta,\alpha} \\ \tilde{f}^{\beta,\alpha} & G_{2,2}^{\beta,\alpha} \end{bmatrix} \quad (\text{A7})$$

$$\hat{G}^{\alpha',\beta} = \begin{bmatrix} G_{1,1}^{\alpha',\beta} & G_{1,2}^{\alpha',\beta} \\ \tilde{f}^{\alpha',\beta} & \tilde{g}^{\alpha',\beta} \end{bmatrix} \quad (\text{A8})$$

$$\hat{G}^{\beta,\alpha'} = \begin{bmatrix} G_{1,1}^{\beta,\alpha'} & \tilde{f}^{\beta,\alpha'} \\ G_{2,1}^{\beta,\alpha'} & \tilde{g}^{\beta,\alpha'} \end{bmatrix}. \quad (\text{A9})$$

We deduce from (29) – (33) and (A4) – (A9) the final form of the Gorkov function in the antiparallel alignment:

$$\begin{aligned}\hat{G}_{\beta,\beta}^{+,-} &= 2i\pi n_F(\omega - \mu_S) \left\{ \rho_f^{\beta,\beta} + |t^{a,\alpha}|^2 g_{1,1}^{a,a,A} \tilde{f}^{\alpha,\beta,A} \rho_g^{\beta,\alpha} + |t^{a',\alpha'}|^2 g_{2,2}^{a',a',A} \tilde{g}^{\alpha',\beta,A} \rho_f^{\beta,\alpha'} + |t^{a,\alpha}|^2 g_{1,1}^{a,a,R} \tilde{g}^{\beta,\alpha,R} \rho_f^{\alpha,\beta} \right. \\ &+ |t^{a',\alpha'}|^2 g_{2,2}^{a',a',R} \tilde{f}^{\beta,\alpha',R} \rho_g^{\alpha',\beta} + |t^{a,\alpha}|^4 g_{1,1}^{a,a,R} g_{1,1}^{a,a,A} \tilde{g}^{\beta,\alpha,R} \tilde{f}^{\alpha,\beta,A} \rho_g^{\alpha,\alpha} + |t^{a',\alpha'}|^4 g_{2,2}^{a',a',R} g_{2,2}^{a',a',A} \tilde{g}^{\alpha',\beta,A} \tilde{f}^{\beta,\alpha',R} \rho_g^{\alpha',\alpha'} \\ &+ |t^{a,\alpha}|^2 |t^{a',\alpha'}|^2 g_{1,1}^{a,a,R} g_{2,2}^{a',a',A} \tilde{g}^{\beta,\alpha,R} \tilde{g}^{\alpha',\beta,A} \rho_f^{\alpha,\alpha'} + |t^{a,\alpha}|^2 |t^{a',\alpha'}|^2 g_{1,1}^{a,a,A} g_{2,2}^{a',a',R} \tilde{f}^{\beta,\alpha',R} \tilde{f}^{\alpha,\beta,A} \rho_f^{\alpha',\alpha'} \left. \right\} \\ &+ 2i\pi n_F(\omega - \mu_a) |t^{a,\alpha}|^2 \tilde{g}^{\beta,\alpha,R} \tilde{f}^{\alpha,\beta,A} \rho_{1,1}^{a,a} + 2i\pi n_F(\omega - \mu_{a'}) |t^{a',\alpha'}|^2 \tilde{f}^{\beta,\alpha',R} \tilde{g}^{\alpha',\beta,A} \rho_{2,2}^{a',a'}.\end{aligned}\quad (\text{A10})$$

Using the renormalized propagators obtained in section III C 1 to evaluate (A10), we can show that Eq. (A10) leads directly to (37) and (38).

3. Two-channel problem with parallel magnetizations

Let us now consider two single-channel ferromagnetic electrodes having a parallel spin orientation. Following section A 2, we obtain

$$\begin{aligned}\hat{G}_{\beta,\beta}^{+,-} &= 2i\pi n_F(\omega - \mu_S) \left\{ \rho_f^{\beta,\beta} + |t^{a,\alpha}|^2 g_{1,1}^{a,a,A} \tilde{f}^{\alpha,\beta,A} \rho_g^{\beta,\alpha} + |t^{a',\alpha'}|^2 g_{1,1}^{a',a',A} \tilde{f}^{\alpha',\beta,A} \rho_g^{\beta,\alpha'} + |t^{a,\alpha}|^2 g_{1,1}^{a,a,R} \tilde{g}^{\beta,\alpha,R} \rho_f^{\alpha,\beta} \right. \\ &+ |t^{a',\alpha'}|^2 g_{1,1}^{a',a',R} \tilde{g}^{\beta,\alpha',R} \rho_f^{\alpha',\beta} + |t^{a,\alpha}|^4 g_{1,1}^{a,a,R} g_{1,1}^{a,a,A} \tilde{g}^{\beta,\alpha,R} \tilde{f}^{\alpha,\beta,A} \rho_g^{\alpha,\alpha} + |t^{a',\alpha'}|^4 g_{1,1}^{a',a',R} g_{1,1}^{a',a',A} \tilde{f}^{\alpha',\beta,A} \tilde{g}^{\beta,\alpha',R} \rho_g^{\alpha',\alpha'} \\ &+ |t^{a,\alpha}|^2 |t^{a',\alpha'}|^2 g_{1,1}^{a,a,R} g_{1,1}^{a',a',A} \tilde{g}^{\beta,\alpha,R} \tilde{f}^{\alpha',\beta,A} \rho_g^{\alpha',\alpha} + |t^{a,\alpha}|^2 |t^{a',\alpha'}|^2 g_{1,1}^{a,a,A} g_{1,1}^{a',a',R} \tilde{g}^{\beta,\alpha',R} \tilde{f}^{\alpha,\beta,A} \rho_g^{\alpha',\alpha'} \left. \right\} \\ &+ 2i\pi n_F(\omega - \mu_a) |t^{a,\alpha}|^2 \tilde{g}^{\beta,\alpha,R} \tilde{f}^{\alpha,\beta,A} \rho_{1,1}^{a,a} + 2i\pi n_F(\omega - \mu_{a'}) |t^{a',\alpha'}|^2 \tilde{g}^{\beta,\alpha',R} \tilde{f}^{\alpha',\beta,A} \rho_{1,1}^{a',a'},\end{aligned}\quad (\text{A11})$$

where the renormalized propagators are given by

$$\tilde{g}^{\alpha,\beta} = \frac{1}{\mathcal{D}_F} \left[g^{\alpha,\beta} + |t^{a',\alpha'}|^2 g_{2,2}^{a',a'} \left(g^{\alpha,\alpha'} g^{\alpha'\beta} - g^{\alpha',\alpha'} g^{\alpha,\beta} \right) \right] \quad (A12)$$

$$\tilde{f}^{\alpha,\beta} = \frac{1}{\mathcal{D}_F} \left[f^{\alpha,\beta} + |t^{a',\alpha'}|^2 g_{2,2}^{a',a'} \left(g^{\alpha,\alpha'} f^{\alpha',\beta} - g^{\alpha',\alpha'} f^{\alpha,\beta} \right) \right] \quad (A13)$$

$$\tilde{g}^{\beta,\alpha} = \frac{1}{\mathcal{D}_F} \left[g^{\beta,\alpha} + |t^{a',\alpha'}|^2 g_{2,2}^{a',a'} \left(g^{\alpha',\alpha} g^{\beta,\alpha'} - g^{\alpha',\alpha'} g^{\beta,\alpha} \right) \right] \quad (A14)$$

$$\tilde{f}^{\beta,\alpha} = \frac{1}{\mathcal{D}_F} \left[f^{\beta,\alpha} + |t^{a',\alpha'}|^2 g_{2,2}^{a',a'} \left(g^{\alpha',\alpha} f^{\beta,\alpha'} - g^{\alpha',\alpha'} f^{\beta,\alpha} \right) \right], \quad (A15)$$

where \mathcal{D}_F is given by Eq. (41). We can show that Eq. (A11) leads directly to (39) and (42).

- [1] P.G. de Gennes, Phys. Letters **23**, 10 (1966).
- [2] G. Deutscher and F. Meunier, Phys. Rev. Lett. **22**, 395 (1969).
- [3] J.J. Hauser, Phys. Rev. Lett. **23**, 374 (1969).
- [4] R. Mélin, J. Phys.: Condens. Matter **13**, 6445 (2001).
- [5] M.J.M. de Jong and C. W. Beenakker, Phys. Rev. Lett. **74**, 1657 (1995).
- [6] P.M. Tedrow and R. Meservey, Phys. Rev. Lett. **26**, 192 (1971);
P.M. Tedrow and R. Meservey, Phys. Rev. B **7**, 318 (1973);
R. Meservey and P.M. Tedrow, Phys. Rep. **238**, 173 (1994).
- [7] M. Tinkham, *Introduction to superconductivity*, Second edition, McGraw-Hill (1996).
- [8] L.V. Keldysh, Sov. Phys. JETP **20**, 1018 (1965).
- [9] C. Caroli, R. Combescot, P. Nozières and D. Saint-James, J. Phys. C: Solid St. Phys. **4**, 916 (1971); *ibid.* **5**, 21 (1972).
- [10] J.C. Cuevas, A. Martin-Rodero, and A. Levy Yeyati, Phys. Rev. B **54**, 7366 (1996).
- [11] A. Martin-Rodero, F.J. Garcia-Vidal, and A. Levy-Yeyati, Phys. Rev. Lett. **72**, 554 (1994).
- [12] R. Mélin and D. Feinberg, arXiv:cond-mat/0106329, submitted to Eur. Phys. J. B (2001).
- [13] A.M. Clogston, Phys. Rev. Lett. **9**, 26 (1962).
- [14] B.S. Chandrasekhar, Appl. Phys. Lett. **1**, 7 (1962).
- [15] P. Fulde, Adv. Phys. **22**, 667 (1973).
- [16] P.G. de Gennes, *Superconductivity of metals and alloys*, W.A. Benjamin (1966).
- [17] R. Mélin, Europhys. Lett. **51**, 202 (2000).
- [18] G. Sarma, J. Phys. Chem. Solids **24**, 1029 (1963).
- [19] K. Maki, Physics **1**, 127 (1964);
K. Maki, Phys. Rev. B **148**, 362 (1966).
- [20] V. Apinaryan and R. Mélin, in preparation.
- [21] N. Moussy, H. Courtois and B. Pannetier, arXiv:cond-mat/0106299.
- [22] S. Guéron, H. Pothier, N.O. Birge, D. Estève and M. Devoret, Phys. Rev. Lett. **77**, 3025 (1996).
- [23] I. Baladié, A. Buzdin, N. Ryzhanova, and A. Vedyayev, Phys. Rev. B **63**, 054518 (2001).
A. Buzdin, A.V. Vedyayev, and N. Ryzhanova, Europhys. Lett. **48**, 686 (1999).